Project Title:

Innovative compact HYbrid electrical/thermal storage systems for low energy BUILDings

Project Acronym:

HYBUILD

Grant Agreement Nº: 768824

Collaborative Project

Deliverable Report

Deliverable number:

D2.4

Deliverable title:

Report on performance tests on the operation of the electrical energy storage

Related task:	2.4
Lead beneficiary:	CNR
Authors and institutions:	CNR - Francesco Sergi, Davide Aloisio, Gianluca Leonardi, Giovanni Brunaccini, Salvatore Micari, Marco Ferraro, Andrea Frazzica, Valeria Palomba
Due date:	M24- 30th of September 2019

DISSEMINATION LEVEL		
PU	Public, fully open, e.g. web	X
CO	Confidential, restricted under conditions set out in Model Grant Agreement	
CI	Classified, information as referred to in Commission Decision 2001/844/EC.	

This project has received funding from the European Union's Horizon 2020 research and innovation programme *under grant agreement No 768824.*
The content of this document reflects only the author's view and the Commission is not responsible for any use that may be made of the information it contains.

DOCUMENT STATUS HISTORY		
Date	Description	Partner
2019/08/29	Draft	CNR
2019/09/06	Reviewed and finalized version	CNR
2019/09/20	Internal quality review completed	UDL, R2M, COMSA

Table of contents

Publishable executive summary **4**

Acronyms and Abbreviations **6**

1 Introduction **7**
1.1 Aims and objectives 7
1.2 Relations to other activities in the project 7
1.3 Report structure 7
1.4 Contributions of partners 8

2 Identification of suitable electric energy storage technologies **9**
2.1 Analysis of dynamic electrical behaviour of the use cases 9
2.2 Evaluation of existing electric energy storage technologies 11
2.2.1 Cathodic materials 13
2.2.2 Anodic materials 15
2.3 Selection of the most appropriate technology 16
2.3.1 Characteristic selection parameters 16

3 Experimental characterization of the selected electric storage technology **24**
3.1 Single module performance and lifetime evaluation tests 24
3.2 BMS adaptation 30
3.2.1 Hardware development 30
3.2.2 Software development activity 31
3.2.3 Firmware development 41
3.3 Battery system development and test in the lab 42

4 Conclusions **47**

5 References **48**

Publishable executive summary

HYBUILD is an EU Horizon 2020 - funded project, led by COMSA Corporación, which will develop two innovative compact hybrid electrical/thermal storage systems for stand-alone and district connected buildings.

The present work describes the activities performed to develop the prototype of the electric energy storage system of the HYBUILD project. The final purpose of the work done was to choose, test, and assemble the electric energy storage system.

The first action performed was to identify the behaviour of the use cases in realistic conditions, considering a wide range of operation. To this aim, the two Mediterranean and Continental systems were considered. In particular, the optimized behaviour for summer conditions (Mediterranean HYBUILD solution) and winter conditions (Continental HYBUILD solution) were taken into account. In the Mediterranean system, the electric storage mainly serves the vapour compression heat pump for cooling production, whereas in the Continental system the electric storage serves the vapour compression heat pump for heating production. Furthermore, in the Mediterranean system, DHW is mainly produced directly from solar or through a back-up, whereas in the Continental system DHW production is obtained through the RPW-HEX accumulating condensation heat of the heat pump during its operation. In both cases, therefore, no extra operation of the heat pump for DHW was considered. A 4.5 kWp system was considered for the Mediterranean solution and a 6 kWp one for the Continental case. This is due to different size of case studies, since the Mediterranean HYBUILD system is intended for a single-family house, while the Continental solution is intended for multi-family houses with 2-3 apartments with shared renewable energy production. Cyprus solar irradiation profile was used for the Mediterranean case and Bordeaux for the Continental one.

The worst-case scenario was considered for testing: in the Mediterranean case, a day in July (high cooling demand), determines an electric consumption of the heat pump of 1.5 kW, corresponding to a heat pump with 5 kW cooling capacity and EER=3.3 (thanks to operation in combination with the sorption module). In the Continental case, a typical winter day was selected, corresponding to very low irradiation and therefore a lower production from the PV field but a higher demand from the user.

After definition of the applications, a selection process among most performing electric storage technologies was performed. In particular, attention was immediately focused on Lithium-ion batteries due to guaranteed performances. Lithium ion batteries offer countless advantages over other types of electrochemical storage such as:

- very high specific energy (Wh/kg) achieving considerable weight and space savings;
- low internal resistance, allowing them to achieve higher currents, therefore charges and discharges at high c-rates, and making them suitable for high power applications;
- limited self-discharge rates, making them the best solution for long-term energy storage;
- no memory effect;
- high lifetime, especially for some specific chemistries;
- high open-circuit voltage (typical values of 3 - 4 V except for lithium titanate where the cell voltage is in the 1.5 V - 2.7V range);
- relatively flat discharge curves (Voltage - SoC) in a wide range of SoCs.

The performance comparison of the technologies already present in the market brought to the choice of LTO (Lithium Titanate Oxide) as possible solution for the considered application in terms of long life and greater safety, no maintenance during lifetime, excellent power density, and good cyclability at high C-rate in both charge and discharge. In particular, the model chosen is a high-energy type, carrying out also a good compromise in terms of energy density.

Preliminary tests at cell and module level were carried out using CNR equipment for battery testing to evaluate performance and achieve a comparative characterization. Tests at different C-rates and operative temperature were performed and results are shown in the report. In particular, a lifetime evaluation was performed with a defined profile to evaluate the degradation. After a 210 days test campaign no degradation was recorded, confirming its appropriateness.

Great effort was spent on the BMS adaption in terms of both hardware and software developments. The main goal was the adaptation of the existing BMU (Battery Management Unit) / CMUs (Cell Management Units) signals exchange (process variables, alarm and failure states, hardware commands) and data structure to the PCS interface (to communicate with the new main controller). This goal implied to develop a system to bidirectionally convert data (i.e. implement the transcoding functions) among a CAN network (within the battery pack/unit) and the Modbus network mastered by the PCS. An Anybus converter by HMS (the "gateway") was selected as the main device of the transcoding system. The gateway exchanges CANbus frames with the BMU, and then it parses, splits, and re-arrange the process variables values into data structures compliant with the Modbus RTU. On the other hand, by acting as a Modbus slave, it receives data from the PCS Modbus line and assemble the data into the CANbus frames compliant with the BMU communication protocol by adding control/header information of the CANbus stream. The software development activity was addressed to implement the transcoding algorithm and the communication between the PCS (from CSEM) and the storage system (from CNR) by synthesizing a common data structure description including the frame timing, signals priorities, system operation limitations to achieve a common FSM (Finite State Machine) implementation. To develop the FSM, a definition of the procedures to implement in case of single status/error/alert/fault coil commutations was realized and described in detail.

After this phase, the whole storage system (3x45Ah LTO modules mounted in series, BMU, protections systems, current sensor, and power supply and communication infrastructure) was cabled for testing and debugging of the control software. The system was arranged to be connected to a DC link in which a dedicated DC/DC converter will impose the current set point (for charge and discharge) following selected algorithm decisions. The electrical layout, including BMS interfaces, power suppliers, wiring, switches and connections was developed in order to achieve a final design for the installation into a cabinet. An external switch for reset, able to restart the storage system when fault conditions are reached, was directly linked to the overall system supervisor (in agreement between CNR and CSEM) to give the total control to it in any operating case.

When the system was ready to be tested, the whole pack was subjected to cycles representing the chosen test days. This test campaign was launched to evaluate the behaviour of the whole system in real operating conditions. The results of the performed tests are shown in the report.

A small electrical cabinet was chosen to ensure right protections (fuses, contactors) to the storage system for testing the DC-Link with CSEM and for achieving a final device to install into the demos. A further external protection system, which bypass the same BMU, was inserted to control the operation inside the rated maximum and minimum voltage limits. The intervention of this protection system occurs in any case, independently from the BMU state, ensuring not over or under voltage operations of the storage system. A necessary pre-charge system needs to be foreseen between the converter and the storage to avoid dangerous voltage unbalance between them.

The objective to obtain a working electric energy storage prototype was achieved by solving all the related issues (hardware and software).

Acronyms and Abbreviations

BMS	Battery Management System
BMU	Battery Management Unit
CMU	Cell Management Units
CNR	National Council of Research (Italy)
DHW	Domestic Hot Water
FSM	Finite State Machine
LCO	Lithium Cobalt Oxide
LFP	Lithium Iron Phospate Oxide
LTO	Lithium Titanate Oxide
NCA	Lithium Nickel Cobalt Aluminium Oxide
NMC	Lithium Nickel Manganese Cobalt Oxide
PCS	Programmable Control System
PV	PhotoVoltaic
SoC	State of Charge

1 Introduction

1.1 Aims and objectives

The goal of this report is to describe the activities done by CNR in designing and developing the electrical storage system for the Mediterranean case study of the HYBUILD project. The activities started with the selection of the right system by choosing a proper chemistry, and continued by the sizing of the same, the cabling process, the right selection and installation of the protections, the communication establishing, the system testing and, finally, the definition of the prototype case. CNR experience on batteries was used to make an overview of the possible candidates (li-ion chemistries) and the proposal of one of them. Afterwards, the sizing of the system was realized by considering two possible case studies (Cyprus for the Mediterranean case, and Bordeaux for the Continental one). On the other side, CSEM worked on the integration of the storage system with the DC-Link by choosing the right converters and realizing the hardware control by a proper developed software, as reported in D2.3. CNR developed a prototype of the storage system and of the communication infrastructur. In particular, great effort was spent on the BMU (Battery Management Unit) communication and battery management. CSEM required the use of a unified communication protocol of all system components. The protocol chosen is MODBUS RTU. The BMU uses CAN protocol to give information about storage status. Hence, a translation between the two protocols, followed by a selection of useful information, was done by choosing and programming a CAN/MODBUS protocol converter. Simultaneously, tests at cell, module and pack level were conducted to obtain information on real behaviour of the technology selected. The prototype is now ready for the installation inside the electrical cabinet, that will be tested in the lab and shipped to the demo sites in the coming months.

1.2 Relations to other activities in the project

The activity presented in this report was carried out within the Task 2.3, aiming at the selection and testing of the electrical storage to be integrated in the final prototype, to be tested in the lab within Task 3.2 and then installed in the demo sites within WP6. Furthermore, it will provide data to WP4 for the control and management of the system as well as to WP5 for the life-cycle analyses.

1.3 Report structure

The report is divided into two main sections: the first one is related to the arguments concerning the evaluation and selection of the proper technology of the prototype; the second section is more focused on the experimental work done to realize and integrate the electric storage system chosen.

The second chapter is divided in three paragraphs:

- Paragraph 2.1 describes the analysis done on the Mediterranean and Continental case needed to identify the electrical request and renewable energy production in worst conditions. This work is useful for sizing the energy storage and to define tests to be done on it to simulate some critical operating days.
- Paragraph 2.2 is a review of commercial li-ion technologies, considered as the most adequate electrochemical system for the application of this project.
- Paragraph 2.3 defines the selection criteria and a comparison of different chemistries features is done to identify and justify the technology selected

The third chapter is divided in three paragraphs:

- Paragraph 3.1 describes test activities performed at cell and module level for the storage system to evaluate performances of the same in terms of capacity at different C-rates and lifetime.
- Paragraph 3.2 is a description of all the activities performed around the BMU (Battery Management Unit). They can be divided into Hardware and Software issues that have been resolved to install and manage the BMU. In particular, the main effort was spent on communication section, by doing extraction and translation of CAN messages to the defined common protocol of the whole system MODBUS RTU, and in the definition of management of all possible event during operation time (faults, warning, critical events etc.)
- Paragraph 3.3 finally is a report of the realization and tests performed on the designed storage system that has to be tested in the lab and installed in the demo site.

1.4 Contributions of partners

The following report was developed by CNR, with the support of CSEM on the realization of the final prototype of the electric energy storage part of the HYBUILD project.

CNR performed various activities on the storage system starting from the choice of the right technology followed by testing and integration of the same in terms of cabling, communication, definition of management in all operation cases, assembling.

2 Identification of suitable electric energy storage technologies

2.1 Analysis of dynamic electrical behaviour of the use cases

Use-cases to be studied and tested were chosen in order to have a meaningful representation of the behaviour of the electric storage in realistic conditions, representative not only of the demonstrators that will be developed within HYBUILD but also of a wider variety of operating conditions. To this aim, the specificity of the two Mediterranean and Continental systems were considered, i.e. the optimized behaviour for summer conditions (Mediterranean HYBUILD solution) and winter conditions (Continental HYBUILD solution). In the Mediterranean system, the electric storage mainly serves the vapour compression heat pump for cooling production, whereas in the Continental system the electric storage serves the vapour compression heat pump for heating production. In the Mediterranean system, DHW is mainly produced directly from solar or through a backup, whereas in the Continental system DHW production is obtained through the RPW-HEX accumulating condensation heat of the heat pump during its operation. In both cases, therefore, no extra operation of the heat pump for DHW is considered.

The electric storage is charged by solar PV panels and discharged when the heat pump needs energy. The size of the solar PV field chosen differs for the two cases: a system with 4.5 kW_p was considered for the Mediterranean solution and a system with 6 kW_p for the Continental one. Such a difference is due to the different optimized sizing of the two solutions: whereas the Mediterranean HYBUILD system is intended for a single-family house, the Continental solution can better exploit a high share of renewables in multi-family houses with 2-3 apartments.

For the calculation of electricity that can be produced from PV panels, solar irradiation in Cyprus and Bordeaux were used. For a plant size of 4.5 kWp and 6 kWp, respectively, the available hourly energy for the entire year is shown in Table 1 and Table 2.

Table 1 - Hourly energy producibility of a PV plant in Cyprus weather conditions. All the values are in kWh

t	4:00	5:00	6:00	7:00	8:00	9:00	10:00	11:00	12:00	13:00	14:00	15:00	16:00	17:00	18:00	19:00
Jan	0	0	0	0,4	0,96	1,51	1,96	2,21	2,21	1,96	1,51	0,96	0,4	0	0	0
Feb	0	0	0	0,69	1,39	2,08	2,63	2,93	2,93	2,63	2,08	1,39	0,69	0	0	0
Mar	0	0	0,26	0,95	1,73	2,48	3,07	3,4	3,4	3,07	2,48	1,73	0,95	0,26	0	0
Apr	0	0	0,43	1,2	2,03	2,81	3,42	3,75	3,75	3,42	2,81	2,03	1,2	0,43	0	0
May	0	0,08	0,5	1,15	1,83	2,47	2,96	3,22	3,22	2,96	2,47	1,83	1,15	0,5	0,08	0
Jun	0	0,11	0,56	1,27	2	2,67	3,19	3,47	3,47	3,19	2,67	2	1,27	0,56	0,11	0
Jul	0	0,09	0,55	1,28	2,05	2,75	3,29	3,59	3,59	3,29	2,75	2,05	1,28	0,55	0,09	0
Aug	0	0,02	0,47	1,21	2	2,74	3,31	3,62	3,62	3,31	2,74	2	1,21	0,47	0,02	0
Sep	0	0	0,3	0,97	1,71	2,42	2,97	3,28	3,28	2,97	2,42	1,71	0,97	0,3	0	0
Oct	0	0	0,16	0,84	1,62	2,38	2,99	3,32	3,32	2,99	2,38	1,62	0,84	0,16	0	0
Nov	0	0	0	0,66	1,4	2,13	2,71	3,04	3,04	2,71	2,13	1,4	0,66	0	0	0
Dec	0	0	0	0,32	0,82	1,33	1,74	1,97	1,97	1,74	1,33	0,82	0,32	0	0	0

Table 2 - Hourly energy producibility of a PV plant in Bordeaux weather conditions. All the values are in kWh

t	4:00	5:00	6:00	7:00	8:00	9:00	10:00	11:00	12:00	13:00	14:00	15:00	16:00	17:00	18:00	19:00
Jan	0	0	0	0,09	0,51	0,95	1,32	1,53	1,53	1,32	0,95	0,51	0,09	0	0	0
Feb	0	0	0	0,41	0,98	1,56	2,04	2,3	2,3	2,04	1,56	0,98	0,41	0	0	0
Mar	0	0	0,19	0,79	1,49	2,17	2,71	3,01	3,01	2,71	2,17	1,49	0,79	0,19	0	0
Apr	0	0	0,47	1,11	1,81	2,47	2,98	3,26	3,26	2,98	2,47	1,81	1,11	0,47	0	0
May	0	0,19	0,71	1,37	2,06	2,7	3,19	3,45	3,45	3,19	2,7	2,06	1,37	0,71	0,19	0
Jun	0	0,26	0,75	1,35	1,96	2,52	2,95	3,18	3,18	2,95	2,52	1,96	1,35	0,75	0,26	0
Jul	0	0,22	0,83	1,59	2,38	3,1	3,64	3,94	3,94	3,64	3,1	2,38	1,59	0,83	0,22	0
Aug	0	0,09	0,68	1,53	2,43	3,26	3,9	4,25	4,25	3,9	3,26	2,43	1,53	0,68	0,09	0
Sep	0	0	0,35	1,09	1,92	2,71	3,34	3,68	3,68	3,34	2,71	1,92	1,09	0,35	0	0
Oct	0	0	0	0,67	1,41	2,15	2,74	3,07	3,07	2,74	2,15	1,41	0,67	0	0	0
Nov	0	0	0	0,23	0,75	1,3	1,75	2	2	1,75	1,3	0,75	0,23	0	0	0
Dec	0	0	0	0	0,73	1,33	1,83	2,11	2,11	1,83	1,33	0,73	0	0	0	0

For the tests of the electric storage modules, a representative daily profile was built, considering the energy produced by the PV field and the electricity demand of the heat pump, according to the typical occupancy behaviour of residential buildings.

For the Mediterranean case, worst-case scenario was considered, i.e. a day in July, when cooling demand (and therefore electricity requested by the heat pump) is significantly high. The overall energy balance on the electric storage (energy produced by PV – energy demand), that was fed as typical user profile during tests is shown in Figure 1. An electric consumption of the heat pump of 1.5 kW, corresponding to a heat pump with 5 kW cooling capacity and EER=3.3 (thanks to operation in combination with the sorption module).

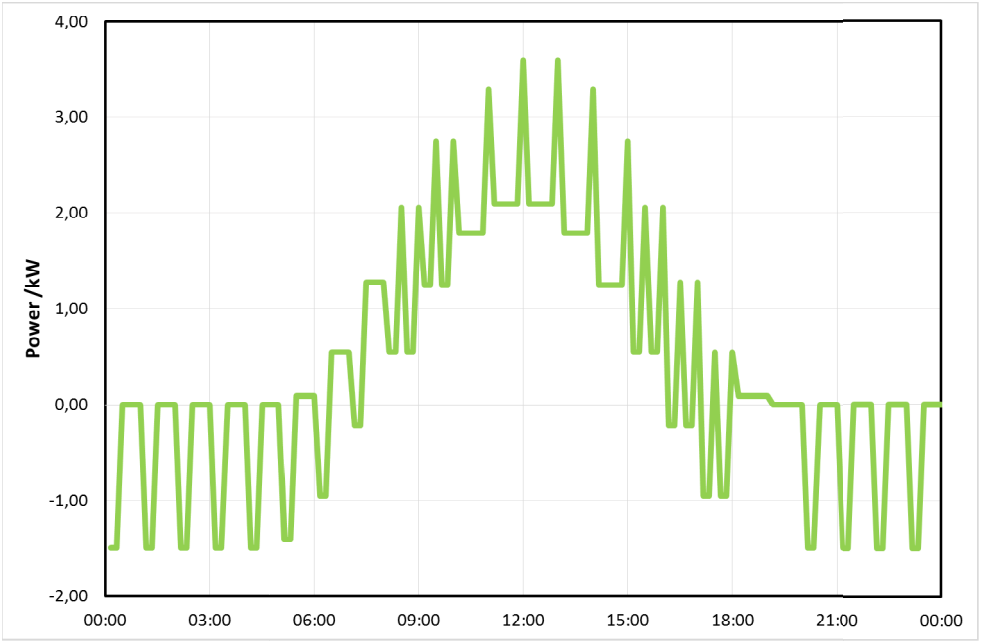

Figure 1 - Use case profile tested - Cyprus, summer

For the Continental case, the worst case corresponds to a typical winter day, in January, in which very low irradiation and therefore a lower production from the PV field are present but

also a higher demand from the user is considered. The resulting use case profile is shown in Figure 2. Response of the electric storage to such user profile is described in section 3.3.

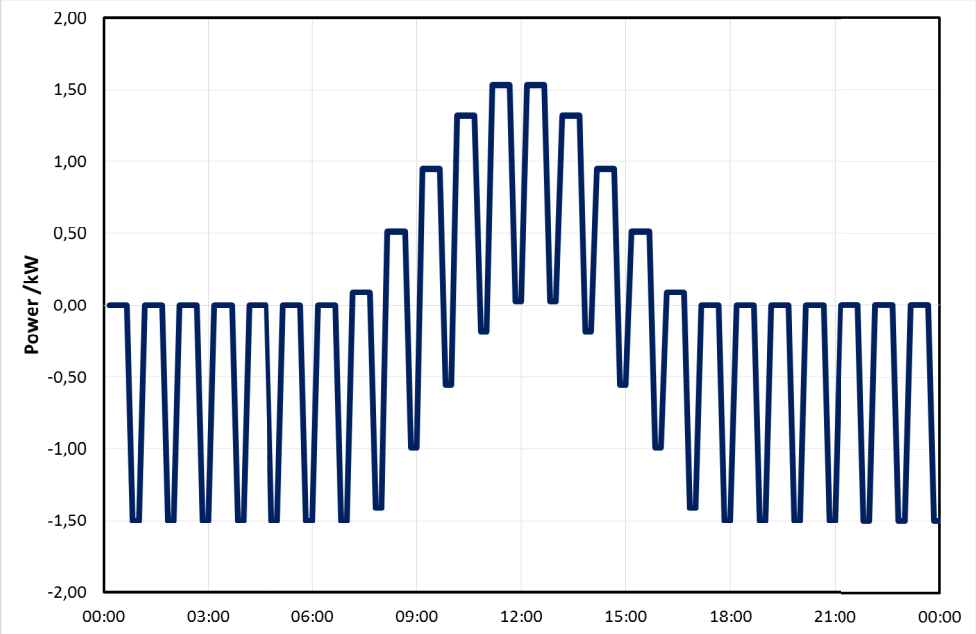

Figure 2 - Use case profile tested - Bordeaux, winter

2.2 Evaluation of existing electric energy storage technologies

Electric energy storage technologies are increasing their appeal year by year in stationary sector due to the need of integration between the electric grid, formerly designed to sustain centralized and well-controlled old fossil-oil-hydro power plants, and new 'floating' renewable energy sources. The worldwide electricity mix nowadays represents on one hand a challenge to be maintained and improved (with a more and more massive renewable sources penetration, while keeping grid parameters stability), and on the other hand an opportunity for the energy storage market. Decentralized storage presence (like batteries integrated with small-scale and domestic solar installations) is increasing in recent year due to greater competitiveness in prices and performance reached, making self-consumption of auto-produced energy more convenient. In addition, new services enabled by these systems can turn the little consumer of renewable energy into an active player in the energy services market, making it the so-called "prosumer". Following this route, small-distributed energy storage systems can take a primary role in the distribution sector, retail and end-use segments [1].

The energy storage system can provide energy-related services or power-related ones. It depends on the ability of the system to store enough energy to answer to the request and on the reactivity in releasing this energy for the selected application. Not all the systems can provide both types of services and in general, they can be divided in 'energy' or 'power' storage systems. Batteries are a flexible solution that can enable both types of services due to volumetric and gravimetric energy density values reached nowadays by some technologies (e.g. Lithium-ion) and fast response times (minutes or second). In particular, the rapid development of these electrochemical storage systems supported also by transportation sector (very increased interests of automotive sector) and subsequent reduction of production costs gave opportunities to use them also for the building sector in conjunction with renewable energy sources.

As previously mentioned, among electric energy storage systems, lithium batteries constitute one of the most promising technology. Batteries with this kind of chemistry, use lithium ions as

active species involved in the redox reactions happening inside the cell and, through processes of intercalation, diffusion and migration within the electrodes and electrolyte, they give rise to flows of current. The basic elements of a lithium ion cell and a simplified representation of the operating principle during discharge are shown in Figure 3.

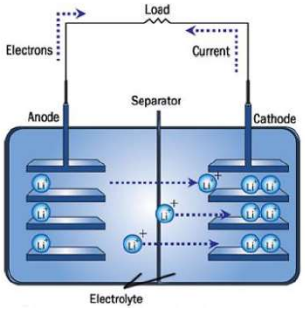

Figure 3 - Schematic representation of the operation of a lithium ion battery during discharge and its main elements

Lithium ion batteries offer countless advantages over other types of electrochemical storage. The main ones are listed below.

- One of the main strengths of lithium batteries is the very high specific energy (Wh/kg). This allows, for the same amount of energy stored, achieving considerable weight and space savings.
- The low internal resistance allows them to achieve higher currents, therefore charges and discharges at high c-rates, which makes them suitable for high power applications and where rapid recharges are required.
- All batteries are subject to energy losses even when not connected to a load. However, lithium ion batteries have limited self-discharge rates compared to other types. This makes them the best solution when long-term energy storage is required.
- Many rechargeable batteries are subject to memory effect, a phenomenon whereby they lose capacity when repeatedly recharged after being only partially discharged. Lithium ion batteries exhibit a limited or almost no memory effect.
- The life of lithium-ion batteries with repeated charge and discharge cycles is considerably higher than other technologies, especially for some specific chemistries
- Lithium ion cells have a higher open-circuit voltage than traditional cells. For example, the typical values of the cell voltage are in the 3 - 4 V range compared to 1.2 - 2 V typical for NiCd, NiMH and lead acid. Except for lithium titanate where cell voltages are in the 1.5 V - 2.7V range.
- Another interesting feature of lithium ion batteries is to present relatively flat discharge curves (Voltage - SoC) in a wide range of SoCs. Consequently, with the same current, they are able to supply an almost constant power during for most of the discharge phase.

Based on the internal chemistry of the cell, it is possible to identify different lithium ion batteries. The main classification is related to the cathode material, according to which it is possible to identify the following types:

- Lithium cobalt oxide ($LiCoO_2$ or LCO);
- Lithium manganese oxide ($LiMn_2O_4$ or LMO);
- Lithium nickel manganese cobalt oxide ($LiNiMnCoO_2$ or NMC);
- Lithium iron phosphate ($LiFePO_4$ or LFP);
- Lithium nickel cobalt aluminium oxide ($LiNiCoAlO_2$ or NCA).

Many of these cathodes are typically associated with a graphite anode. Recently, the use of an alternative material such as titanium oxide has been introduced. When a lithium ion battery uses this type of anode material it is indicated as Lithium titanate (LTO).

Finally, the batteries can be identified based on the electrolyte, which can be liquid or solid (polymeric). In the latter are indicated as Lithium-polymer.

As previously seen, most cathode intercalation materials are based on metal oxides such as Mn, Ni, Co and Fe. This is due to the great stability and the high half-cell potential, which gives them a great energy storage capacity. Typically, the intercalation cathodes can have a specific capacity of 100-200 mAh/g and an average voltage of 3.5 - 4.5 V with respect to the Li/Li + pair [2] (Figure 4).

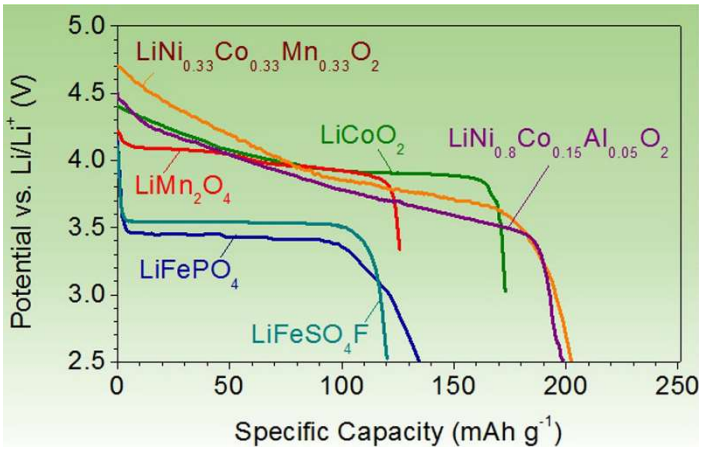

Figure 4 - Typical discharge profile, potential (V vs Li/Li^+) - specific capacity (mAh/g) of intercalation cathode materials [2]

A brief description of the most important materials and technologies of Lithium-ion batteries is given below.

2.2.1 Cathodic materials

- Lithium cobalt oxide (LCO)

$LiCoO_2$ (LCO) is one of the first materials used as a cathode for lithium ion cells. Initially marketed by SONY, it is still widely used today in many batteries. LCO is a very attractive cathode material due to its high specific and volumetric theoretical capacity of 274 mAh/g and 1363 mAh/cm^3 respectively, high semi-cell tension and excellent redox cycle reversibility. The main limitations are related to the high cost of cobalt, low thermal stability and loss of capacity with deep charge-discharge cycles. Thermal instability is generally referred to the exothermic release of oxygen when a lithium-metal oxide cathode is heated beyond a certain threshold. Under these conditions, gas could be released with the consequent risk of explosion or flame generation. From this point of view, the LCO has a lower thermal stability than other similar cathode materials, although it also depends largely on factors related to the design and the dimensions of the cell. Deep charging of cathode-based batteries on LCO could result in excess lithium removal from the structure resulting in lattice distortion and loss of performance.

- Lithium nickel cobalt aluminum oxide (NCA)

$LiNiO_2$ (LNO) has a crystal structure very similar to LCO and a comparable theoretical specific capacity of 275 mAh/g. The performance, in terms of capacity and accumulated energy, very similar to the LCO would indicate LNO as the most advantageous thanks to the lower cost. However, the cathodes of LNO are much less chemically and thermally stable than the

previous ones, limiting their use in pure form. Co doping is a very effective solution to reduce lattice instability, and the addition of additional dopants such as Mg and Al are often used to improve both thermal stability and electrochemical performance. For these reasons, $LiNiCoAlO_2$ (NCA) has found wide commercial use compared to the simple LNO, being also able to represent a valid alternative to the LCO cathodes thanks to the sufficiently high theoretical specific capacity of 200 mAh/g. Cells with cathode in NCA have been developed in collaboration between Panasonic and Tesla for applications on electric vehicles. However, it is well known that cathodes with this particular composition are subject to a significant loss of capacity when they are working at a temperature higher than 40 °C, requiring, in many cases, the use of adequate cooling systems. Furthermore, they show a marked tendency to thicken the solid-electrolyte interface and the formation of micro-cracks at the edges of the grains that affect its performance. In fact, is quite common for lithium batteries that, during the charging and discharging cycles of a battery, there is the formation and growth of a passivation layer on the surface of the electrodes in contact with the electrolyte. The thickening of the latter reduces the spread of lithium with a consequent increase of the internal resistance of the cell and loss of capacity. At the same time, the presence of this layer at the interface is necessary because it limits the dissolution of the electrodes extending their lifetime. Consequently, any phenomenon that causes its damage, as well as the formation of micro-cracks, reduces the life of the electrode.

- Lithium manganese oxide (LMO)

$LiMnO_2$ (LMO) could be very promising because Mn is much cheaper and less toxic than both Co and Ni. However, the resistance to repeated charging and discharging cycles of cathodes in LMO is not excellent since the structure, initially stratified, tends to become spinel during the extraction of Li ions. Even using directly cathodes in LMO with spinel structure, there are only limited improvements on long-term reversibility. In fact, it presents a rapid decline in performance having the tendency to react with the electrolyte, to lose oxygen and manganese from the lattice and to form new phases, especially at high c-rates.

The stabilization of the cathode in LMO is however obtainable by doping it with Co and Ni ions. The $LiNiCoMnO_2$ (NMC) cathodes have similar or even higher specific capacities than those obtainable with LCO and analogous operating voltages despite having a lower cost since the Co content is reduced. The most common form of NMC, widely used in commercial batteries, is the $LiNi_{0.33}\ Co_{0.33}\ Mn_{0.33}O_2$ type. For this specific composition the values of theoretical specific capacity of 234 mAh/g, good thermal stability up to over 200 °C and voltages higher than 4.5 V (vs Li/Li^+) are reported.

- Lithium iron phosphate (LFP)

Among the most recent materials used for the construction of lithium battery cathodes polyanionic compounds can be found. These are crystal structures in which some reticular positions are occupied by anions (sulfur, phosphorus, silicon, etc.), which confer excellent electrochemical performance and stability to the crystal lattice. Among the various materials belonging to this class, the olivine lithium iron phosphate ($LiFePO_4$) was the most promising for the construction of lithium ion cell cathodes and is currently the only composition used in commercial batteries. The main advantages lie in its thermal stability and its ability to withstand high current densities. When used as a cathode material in batteries, the best thermal stability makes them less susceptible to explosion or flame generation in case of over-charging or short-circuit. The main limitations of the cathode in LFP are due to the relatively lower potential compared to other materials, to the energy density which is much lower if compared with the LCO-based cathodes and to the low electrical conductivity when used as it is. This last aspect could significantly affect the performance of the cell, for example by limiting the c-rate. However, in order to increase the electronic conductivity and generally improve the

electrochemical performance of the cathode in LFP, some strategies are adopted. One of the most common practices implemented in commercial cells is to mix or coat the positive electrode with carbon. Recently, it has also been shown that the reduction of the particles size constituting the electrode material (nano-phosphate cells) and the cationic doping, in combination with the carbon coating, allows reducing the resistance of the material favoring the release of high currents and consequently a higher power.

2.2.2 Anodic materials

In addition to the importance of cathode materials, an important contribution to performance of li-ion batteries is also linked to the anode composition. In principle, to be suitable for the production of lithium ion batteries, anode materials should meet the following requirements:

- guarantee high energy density;
- provide high cell voltage when coupled to the cathode (small half-cell potential);
- high conductivity;
- long lifetime;
- reduced weight;
- low cost;
- environmental compatibility.

The pure metallic lithium from a theoretical point of view would be the best anodic material. However, the rapid growth of dendritic structures during the charge cycles could cause a short circuit inside the cell, with consequent serious safety issues. Currently, graphite is the material almost exclusively used as the anode of secondary lithium batteries. Other anodic materials have been proposed as an alternative to graphite that seem promising in terms of maximum achievable cell voltage and specific capacity Figure 5 [3]. Despite all this, to date only lithium titanate (LTO) is an alternative material to graphite in the production of commercial lithium ion batteries.

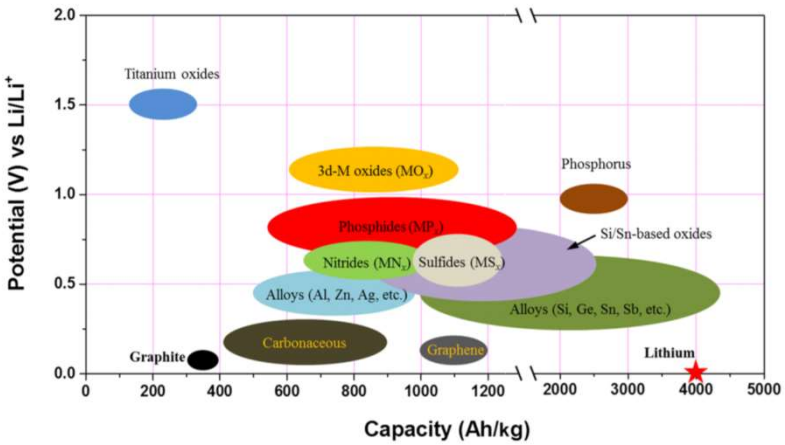

Figure 5 - Potential (V vs Li/Li^+) - specific capacity (Ah/kg) of commercial and alternative anode materials [3]

- Graphite

Carbon-based materials are the most widespread for the construction of commercial lithium ion cells due to their physical, chemical and low-cost characteristics. In fact, carbonaceous materials have a high electrical (~10^{-4} S/cm) and thermal conductivity (~3000 W/mK), high specific capacity up to 370 mA/g, wide availability and excellent environmental compatibility. Furthermore, since lithium ions bind more weakly to graphite than metal oxides, the intercalation and de-intercalation processes are energetically favored.

Commercial carbon anodes can be divided into:

- graphite;
- Hard carbon.

Graphitic carbons, consisting of large grains of graphite, are well known because they can reach almost the entire theoretical charge capacity when used in the cell. However, they easily react with the electrolytes used in lithium ion batteries leading to the exfoliation of graphite, which, together with the normal formation of a passivation layer at the solid-electrolyte interface (SEI-Solid Electrolyte Interphase), contributes to the loss of capacity.

Hard carbon is made up of small graphitic grains with the main difference from the previous materials being less susceptible to exfoliation. These grains also have nano-voids, which favor the volumetric expansion of the anode during the intercalation of the lithium to the advantage of cyclical duration. However, compared to the previous type of carbon, they have a greater propensity towards the formation of SEI with consequent and more accentuated loss of capacity already during the first cycles.

- Lithium titanate (LTO)

Lithium titanate anodes (LTO) are currently the only commercial alternative to graphite, thanks to better thermal stability and above all excellent durability when subjected to charge-discharge cycles. This feature arises from the fact that during the phase change, in intercalation process, the LTO undergoes only a slight variation in volume (about 0.2%) which gives it excellent mechanical stability compared to graphite. Furthermore, the high half-cell potential (1.55 V vs. Li/Li^+) allows the LTO to operate at such a potential that the growth of the SEI to the anode is significantly reduced. Even when this solid-electrolyte interface is formed, the reduced deformation of the anode due to the change in volume limits its cracking, making the whole cell more stable. A further advantage linked to the high potential of the LTO is the prevention of deposition of metallic lithium with consequent formation of dendrites that would short-circuit the cell internally. This feature allows charging the anode batteries in LTO much more quickly than the others even at temperatures below 0°C. However, the high potential of this material is the main limiting factor in performance. In fact, using the same cathode and replacing the graphite anode with LTO, the cell voltage is lower compared to the first case even more than 1.0 V. Moreover, the specific capacity equal to only 175 mAh/g in association with the low cell voltage results in a lower energy storage. In general, when high life cycles and greater safety are required, the anode in LTO is preferable to graphite.

2.3 Selection of the most appropriate technology

Each battery has different characteristics and performances that are mainly determined by the chemical composition, structural design and dimensions. The selection of a battery consists in finding the right combination of these characteristics in order to meet the needs required by a specific application. In most situations, the choice of batteries is carried out according to six selection criteria, three of which are based on operational and functional performance such as capacity, power and lifetime, while the other three are related to costs, safety and dimensions. The cost is very often the factor that has the greatest weight in the selection. However, in applications related to the building sector, the safety and the lifetime are also very important aspects. Regarding safety, there are specific regulations and guidelines to be followed for the correct installation and use of batteries on buildings.

2.3.1 Characteristic selection parameters

- Capacity

The capacity of a battery is the maximum electrical charge that can be stored and is often measured in Ampere hours (Ah). From the application point of view, it is, however, more interesting to refer to the maximum storable energy expressed in Watts per hour (Wh). This is

related to the fact that different batteries can have a different cell voltage, therefore, with the same Ah, the one with lower voltage will have a lower energy storage capacity. To compare batteries with different chemistries, the "energy density" parameter is often used, which can be gravimetric (Wh/kg) or volumetric (Wh/l). Average energy density values for the various rechargeable battery technologies can be found in the range 40 Wh/kg - 200 Wh/kg. The capacity is determined by the amount of energy that can be stored in the electrode, therefore, in principle, an electrode thicker or with more mass determines a greater capacity. In reality, the amount of energy accumulated by a battery is closely related to the materials constituting the electrodes. In fact, it is mainly dependent on their different ability to store charge, which in turn is linked to their lattice structure. For example, in the case of lithium batteries, an electrode material consisting of a reticular structure capable of accommodating a large number of lithium ions will increase the accumulated energy reserve. Even the electrolyte affects the energy capacity of a battery. In fact, it must possess good ability in transferring charge, limiting losses as much as possible, in order to fully exploit the total energy storage capacity of the battery. Since the electrolyte also contributes to the total mass, its lower density or the possibility of reducing the number of cell components would result in an increase in the specific capacity (Wh/kg) and volumetric (Wh/l). In addition to weight, space is an aspect of fundamental importance to take into consideration in applications in which space availability could be a problem.

- Power

Gravimetric (W/kg) or volumetric (W/l) power density is used to compare different batteries. High nominal power values are necessary in all those situations where rapid loads are required or when it is necessary to compensate for load power peaks.

Lithium ion cells [5] are the most suitable technologies for power density. This is because, depending on the chemical specification, they could be capable of delivering high power (LTO, LFP), or guaranteeing high-energy storage capacity (Li-Polymer). In order to guarantee high power, the chemical and charge transfer processes must have the lowest possible resistance. A low internal resistance is generally obtained by using electrodes of small thickness and a large active surface. Unfortunately, this is in contradiction with what is required to have a high-energy capacity. Therefore, it is always necessary to find a balance for the right combination of capacity and power.

- Lifetime

The lifetime of a battery is determined by two different aging conditions called "calendar life" and "cycle life". While the calendar life is linked to the normal loss of capacity over time regardless its use, the cycle life takes into account the loss of capacity due to the number of charge-discharge cycles during use. Aging, in both cases, is due to alterations in the chemistry of the electrodes and electrolyte (e.g. loss of lithium, formation of surface layers, deterioration of the electrode, dissolution of the materials, and reduction of the contact surface).

To reduce aging and increase durability, electrode base materials are usually mixed with additional substances, although this very often results in a loss of battery performance.

- Safety

Safety is another decisive factor in the choice of batteries: safety is linked to the reliability of every part such as the terminals, the case, any vents and each element constituting the individual cells.

As with any other battery, even lithium-ion technology, due to the substances contained inside the cell could present some chemical risks. Although they are designed to not release any

substance during normal conditions of use, due to accidental causes, e.g. mechanical damage, explosions, etc., this could happen. In this case, two conditions must be assessed [7]:

- Risk related to the corrosive and inflammable properties of the electrolyte;
- Risk related to the toxicity or flammability of volatile organic substances.

Beyond the chemical risk, one of the most significant criticalities of lithium ion batteries is considered the thermal escape (Thermal run-away). This phenomenon is nothing more than a thermal instability caused by an uncontrolled chemical reaction that triggers at the level of a single cell and then propagates inside an entire battery module. Different events could lead to this phenomenon of thermal instability, such as external or internal short-circuit, over-charging, too high operating temperatures reached, overheating from external sources, mechanical damage and BMS failure. Therefore, this type of problem requires special protection systems in addition to the necessary precautions during use.

The mechanism that leads to the thermal escape is usually associated with the degradation of the passivation layer (SEI) that mainly covers the surface of the negative graphite electrodes and the consequent release of carbonaceous species in the electrolyte [7]. In fact, when the temperature inside the cell exceeds 80 °C due to any external cause, the SEI starts a progressive dissolution in the electrolyte, giving rise to exothermic reactions with the latter, therefore releasing heat. The further increase in temperature involves electrodes, the separator and any other parts of the cell in the exothermic process, which, causing a rapid acceleration of the process itself, could lead to the release of gas, fire ignition or the explosion of the battery.

Depending on the cell chemistry, the ignition temperature and the propagation speed of the reactions leading to the thermal run-away can change. For example, as regards the anode, the replacement of graphite with lithium-titanate (LTO) eliminates the problem of the reactivity of carbon with electrolyte, minimizing the risk of ignition of the thermal run-away. At the same time, the improved mechanical stability of the LTO anode avoids SEI fracturing by limiting the direct interaction of the electrode's active material with the electrolyte, reducing its dissolution and oxygen release. The characteristics conferred by this type of chemistry make it one of the safest batteries among the various lithium technologies. As for the cathode, the main problem is related to the decomposition of metal oxides with consequent release of oxygen, which, in addition to acting as an oxidizing for the electrolyte, could increase the pressure inside the cell with a consequent risk of explosion. For example, LCO batteries have a strong tendency to go on a thermal run-away. This is due to the decomposition of the cathode material already for temperatures slightly above 150°C. However, the use of mixed metal oxides, as in the case of NMC cells, improves thermal stability by increasing the cathode decomposition temperature over 220-280 °C [8][9]. Among the various cathode materials, lithium iron phosphate (LFP) is considered as the safest one due to its thermal stability up to over 250 °C and the reduced release of oxygen during decomposition [10].

The first step in the selection process is the determination of the basic requirements such as for example the minimum energy storage and the maximum deliverable power. In this regard, the batteries can be divided into high power and high energy. In application related to buildings there is in general less need of high-power performances. However short charging time (and consequently high C-rate charging) can be useful when high difference between production and request is present. Conversely, the time energy release during typical operation can be considered a long-range request (hours, day, and months), so in this case high-energy cells are preferable.

Once the basic requirements have been defined, a compromise must be found between the maximum capacity to be installed and the maximum power that can be supplied and both have to be balanced as a function of costs.

The last step in the selection process is the integration of the battery system into the whole plant. This step concerns the physical positioning of the batteries in order to respect the safety, functional and performance requirements of the entire system. The physical positioning of the batteries is mainly influenced by the size and weight of the entire system. The choice of the type of battery in terms of both chemistry and shape can greatly affect these two parameters. For example, different types of batteries may have different security needs. This is translated into specific requirements for electrical protection, fire protection and thermal management systems that could affect the costs, weights and dimensions of the system.

Figure 6 shows the radar diagrams of the main features of the six most common chemistries for lithium ion batteries [11][12].

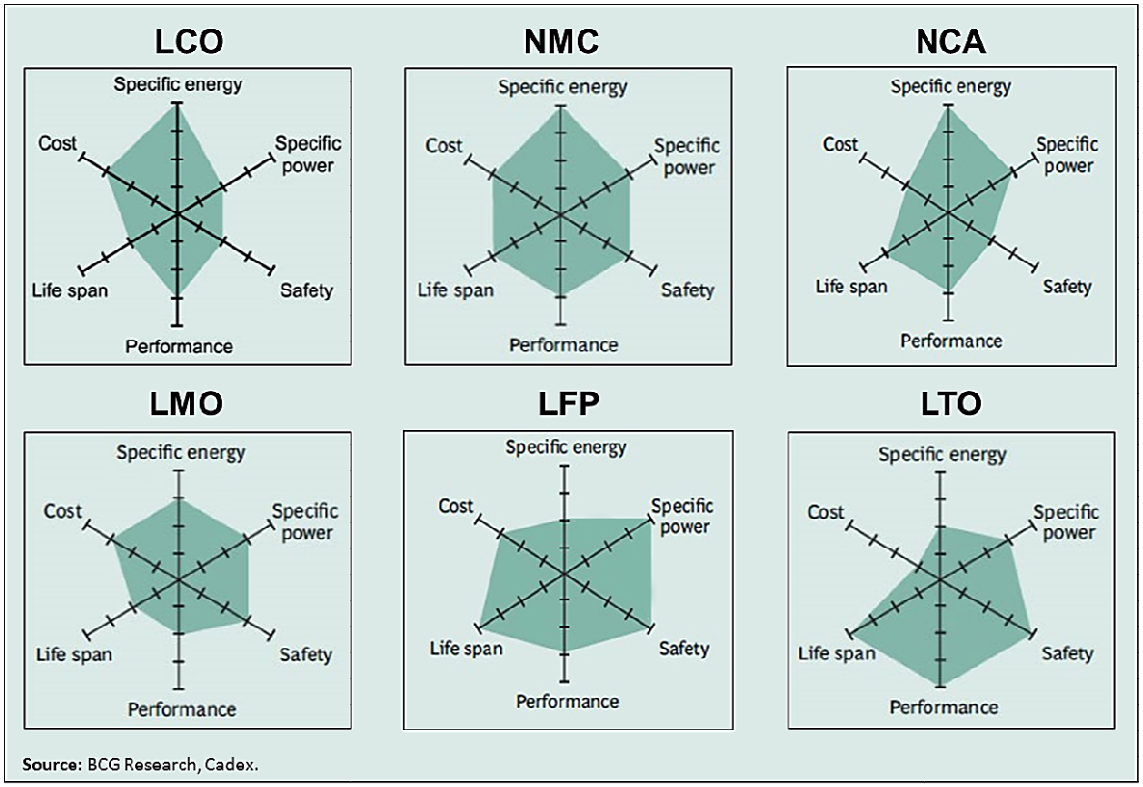

Figure 6 - Radar diagrams of the characteristics of six of the main types of lithium ion cells [5]

LCO

The LCO cells normally have high specific energy; however, due to the high cost, the tolerable low c-rates and the limited safety, they have been almost completely replaced by other chemistries such as NMC and NCA, in which the typical performances of the LCO are maintained or improved.

Advantages:

- High cell voltage;
- High specific energy;
- Sufficient number of life cycles (at 1C discharge): more than 500 cycles;
- High energy efficiency of charge / discharge: 90%;
- They don't suffer from the memory effect

Disadvantages:

- High cost;
- Safety problems in case of overheating or overload;
- Charge at low or high temperature not recommended.

LMO

LMO cells use a cathode based on manganese oxide, which, being a material much more available and cheaper than cobalt, for example, allows to reduce the overall cost of the battery.

Advantages:

- High cell voltage;
- High energy efficiency of charge / discharge: 90%;
- Low cost;
- They don't suffer from the memory effect.

Disadvantages:

- Limited number of life cycles: <500-700;
- Relatively low specific energy;
- Charge at low or high temperature not recommended.

NMC and NCA

NMC and NCA cells are an evolution of the LCO and LMO cells. The addition of nickel in combination with manganese (NMC) and possibly aluminum (NCA) make it possible to reduce the amount of cobalt used, thus lowering costs.

Advantages:

- High cell voltage;
- High energy density;
- High energy efficiency of charge / discharge: 90%;
- Number of relatively high life cycles: more than 1000 (per NMC);
- Do not suffer from the memory effect;

Disadvantages:

- Charge at low or high temperature not recommended;
- Number of limited life cycles: about 500 (for NCA).

LFP

LFPs are one of the latest technologies in lithium ion batteries. The excellent tolerance of high c-rates makes it one of the main choices in applications where high power is required. The lower rated voltage compared to other chemistries and the lower specific energy are the limiting factors of this type of battery.

Advantages:

- High charge / discharge currents;
- They allow faster charges than other types;
- High number of life cycles: more than 1000;
- Greater safety thanks to better thermal stability;
- High energy efficiency of charge / discharge: 95%;
- Do not suffer from the memory effect;

Disadvantages:

- Less cell voltage;
- Low specific energy;
- Charge at low or high temperature not recommended.

Li-Poly

The lithium-polymer cells combine the advantages of cobalt-based cathodes with a polymeric electrolyte that guarantees structural flexibility and savings in terms of volume and weight.

Advantages:

- High specific energy;
- High energy / volume ratio;
- High power density;
- Charge / discharge efficiency ≥95%;

Disadvantages:

- Relatively high cost;
- Number of life cycles dependent on the cathode used.

LTO

LTO batteries are the latest fully validated and commercialized lithium ion technology. The main advantage lies in the fact that the replacement of the graphite anode with lithium titanate confers a significantly higher life cycle than all other technologies. In addition, LTO cells can be charged quickly, at low temperatures and are considered the safest lithium technology. The most important limitations are related to the high cost, low cell voltage and reduced specific capacity.

Advantages:

- High number of life cycles:> 16000
- High charging currents: equal to 1 ÷ 5 C;
- High power density;
- High discharge currents: 5 ÷ 10 C;
- They tolerate temperature stress;
- Excellent safety;
- Possibility of charging at temperatures below 0 ° C;

Disadvantages:

- High cost;
- Low specific energy;
- Low cell voltage.

Table 3 compares the typical values of the main parameters for commercial lithium ion cells [12][13].

Table 3 - Comparison of different lithium ion cells

	LCO	LMO	NMC	NCA	LFP	LTO	Li-polimer
Rated Voltage (V)	3.60	3.70-3.80	3.60-3.70	3.60	3.20-3.30	2.40	3.6-3.75
Specific Energy (Wh/kg)	150- 240	100-150	150-220	200-260	90-130	50-100	100-260
Energy Density (Wh/l)	~560	~420	~580	~460	240-300	170-200	250-350
Power Density (W/kg)	150-3000	150-300	~1800	-	200-2700	1400-5000	700-2800
Cost (€/kWh)	370-1800				350-1400	1200-3000	1300-1800
Max continuous charge C-rate	0.7–1C	1C	1-3C	0.7C	1-1.5C	1-4C	1-2C
Max continuous discharge C-rate	1C	1-6C(pulse)	1-6C	1C	1-25C(pulse)	10-30C(pulse)	5C
Monthly self-discharge (%)	5	5	5	5	5-8	5	5
Cycles lifetime until 80% of initial capacity	500+	300+	1000-14000	~500	1000-3000	16000-60000	6000-10000
Operative Temperature	-30 - 60°C Charge >0°C	-30 - 60°C Charge >0°C	-30 - 60°C Charge >0°C	-30 - 60°C Charge >0°C	-40 - 50°C Charge >0°C	-40 - 55°C Charge <0°C	-20 - 60°C Charge >0°C
Safety	Deep charging promotes thermal runaway (150°C)	Deep charging promotes thermal runaway (250°C)	Deep charging promotes thermal runaway (210°C)	Deep charging promotes thermal runaway (150°C)	Very safe even with deep charges and discharges (270°C)	Very safe in different operating conditions Thermal escape linked to the cathode	Polymeric electrolyte promotes thermal escape

In terms of costs/benefits, considering the long life and greater safety, no maintenance during life time, excellent power density, good cyclability at high C-rate both in charge and discharge, the choice of LTO battery has been considered a possible solution for the selected applications. In particular, the model chosen is a high-energy type, carrying out also a good compromise in terms of energy density.

Main features for the cell and the module are reported in the figures below.

These battery modules have been acquired and tested at CNR-ITAE.

Cell Electrical Characteristics	
Nominal Voltage (V)	2.3
Rated Capacity (Ah)	23
Rated Energy (kWh)	0.046
Vol. Energy density (Wh/L)	202
Nominal Current (A)	23
Cell mechanical Characteristics	
Size (LxWxH) (mm)	116x22x106
Weight (g)	≈ 550

Figure 7 - LTO cell and main characteristics

Module Electrical Characteristics	
Nominal Voltage (V)	27.6
Rated Capacity (Ah)	45
Rated Energy (kWh)	1.242
Upper cut-off Voltage (V)	32.4 (2.7 V cell)
Lower cut-off Voltage (V)	18 (1.5 V cell)
Nominal Current (A)	45
Max Current (A)	160 (Cont.) 350 (peak)
Module mechanical Characteristics	
Size (LxWxH) (mm)	190x361x125
Weight (kg)	15
Module environmental working range	
Temperature range (°C)	-30/55

Figure 8 - LTO battery module and main characteristics

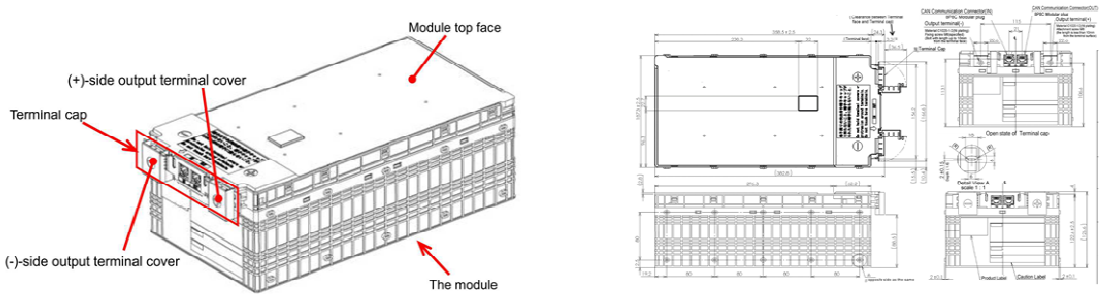

Figure 9 - Schematic view of the battery module

3 Experimental characterization of the selected electric storage technology

3.1 Single module performance and lifetime evaluation tests

In order to investigate the performance of the selected electrical storage system, a characterization of both single cell and module was performed.

All the tests were carried out in a climate chamber (model Angelantoni Discovery DM340 T BT) which allows an accurate control of the temperature. Electrical measurements were carried out by a potentiostat Autolab 302N and a battery cycler Arbin EVTS-X for cell and module, respectively (Figure 10 and Table 4).

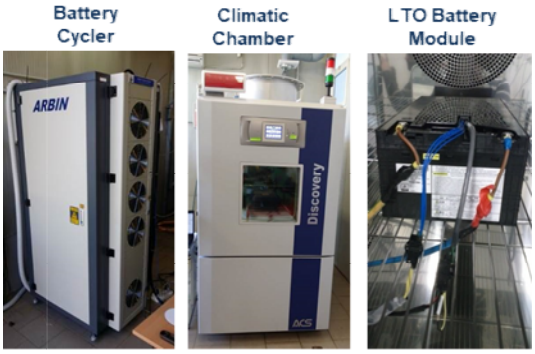

Figure 10 - Battery cycler, climatic chamber and battery module

Table 4 - Main characteristics of the instrumentation used for the battery test

Climatic Chamber Angelantoni Discovery 600L ➢ Safety degree EUCAR 6 ➢ Temperature range: -40 °C - +180 °C ➢ Humidity range: 10% - 98% (+5 °C - +95 °C) ➢ Internal dimensions: 850x740x890 mm
Battery cycler Arbin Instruments EVTS-X ➢ Number of Circuits: 1 ➢ Max Power 30 kW ➢ Voltage range: 0-150 V ➢ Voltage Resolution: 0.15 V ➢ Max Current: 200 A ➢ Current Ranges: 200 A; 25 A ➢ Current Resolutions: 0.2 A; 0.025 A
Potentiostat Autolab PGSTAT302N / BOOSTER20A ➢ Number of Channels: 1 ➢ Potential range +/- 10 V ➢ Maximum current 2 A (20 A with BOOSTER20A) ➢ Current ranges 1 A to 10 nA ➢ Potential resolution 0.3 µV ➢ Input impedance > 1 TOhm ➢ Frequency range 10 µHz - 1 MHz

Figure 11 shows the voltage profiles of a single LTO cell, constituting the module, recorded during charge and discharge steps at different C-rates (1-0.75-0.5-0.25 C, considering nominal C-rate C=45Ah) and 25 °C.

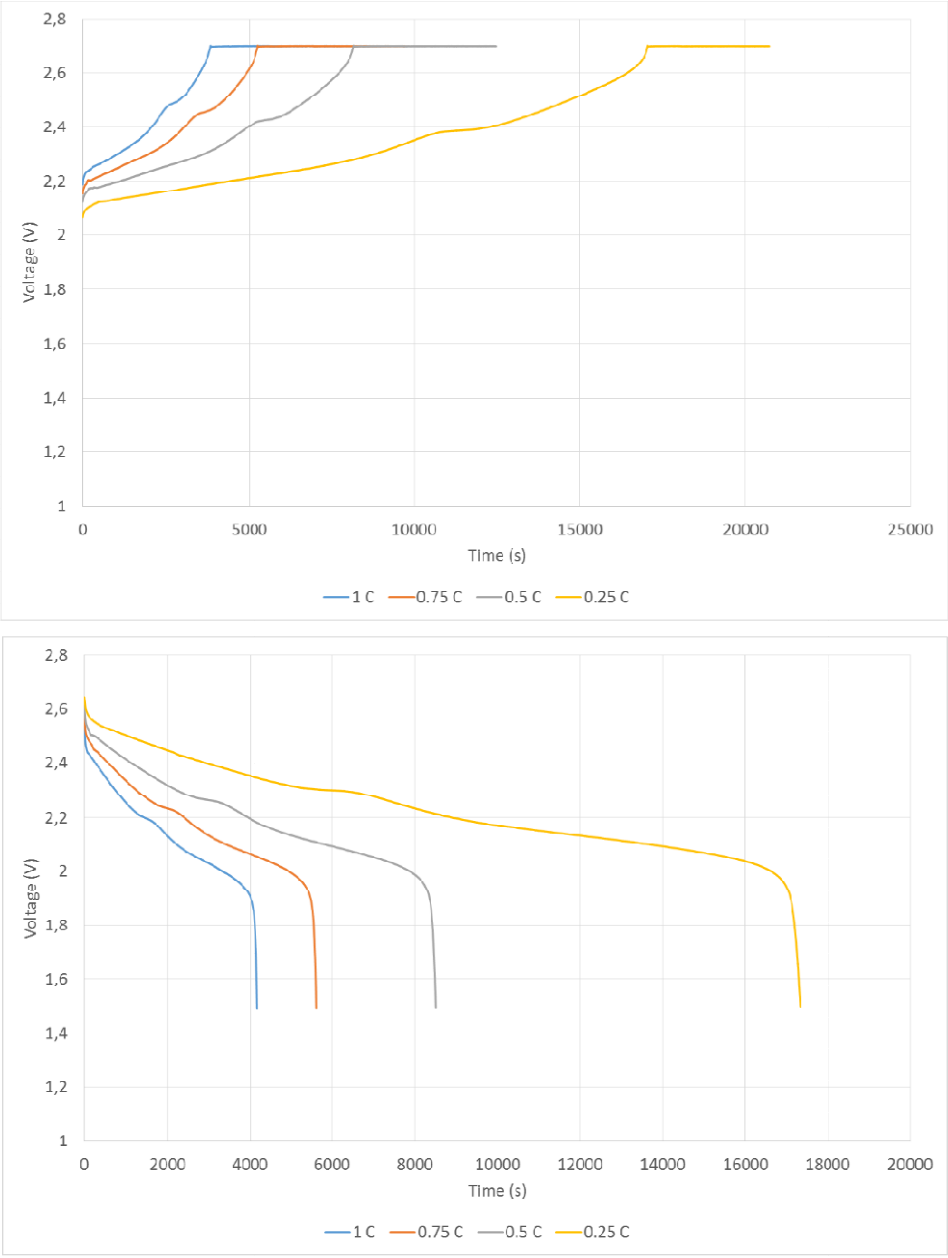

Figure 11 - Charge and discharge voltage profiles at different C-rate and 25 °C of the single cell

Charging step was performed according to a galvanostatic-potentiostatic protocol. It consisted of a constant current (CC) charge up to upper cut-off voltage of the cell (2.7 V) and a final potentiostatic charge at fixed voltage (CV), until the threshold limit current of 0.01 A was reached. Discharge step was performed at constant current up to the lower cut-off voltage of the cell (1.5 V).

As can be observed, at different C-rates the voltage profiles are very similar. Slope variations of the curve, due to the phase transformation processes of anodic and cathodic materials as effect of lithium intercalation and de-intercalation from the electrodes, are well visible for each c-rate. The difference of charge and discharge times is only due to the current adopted during the galvanostatic phase (different c-rates).

Figure 12 compares the voltage profiles recorded during charge and discharge of the cell at 0.5 C and operating temperature of 25°C, 35°C, and 45°C respectively.

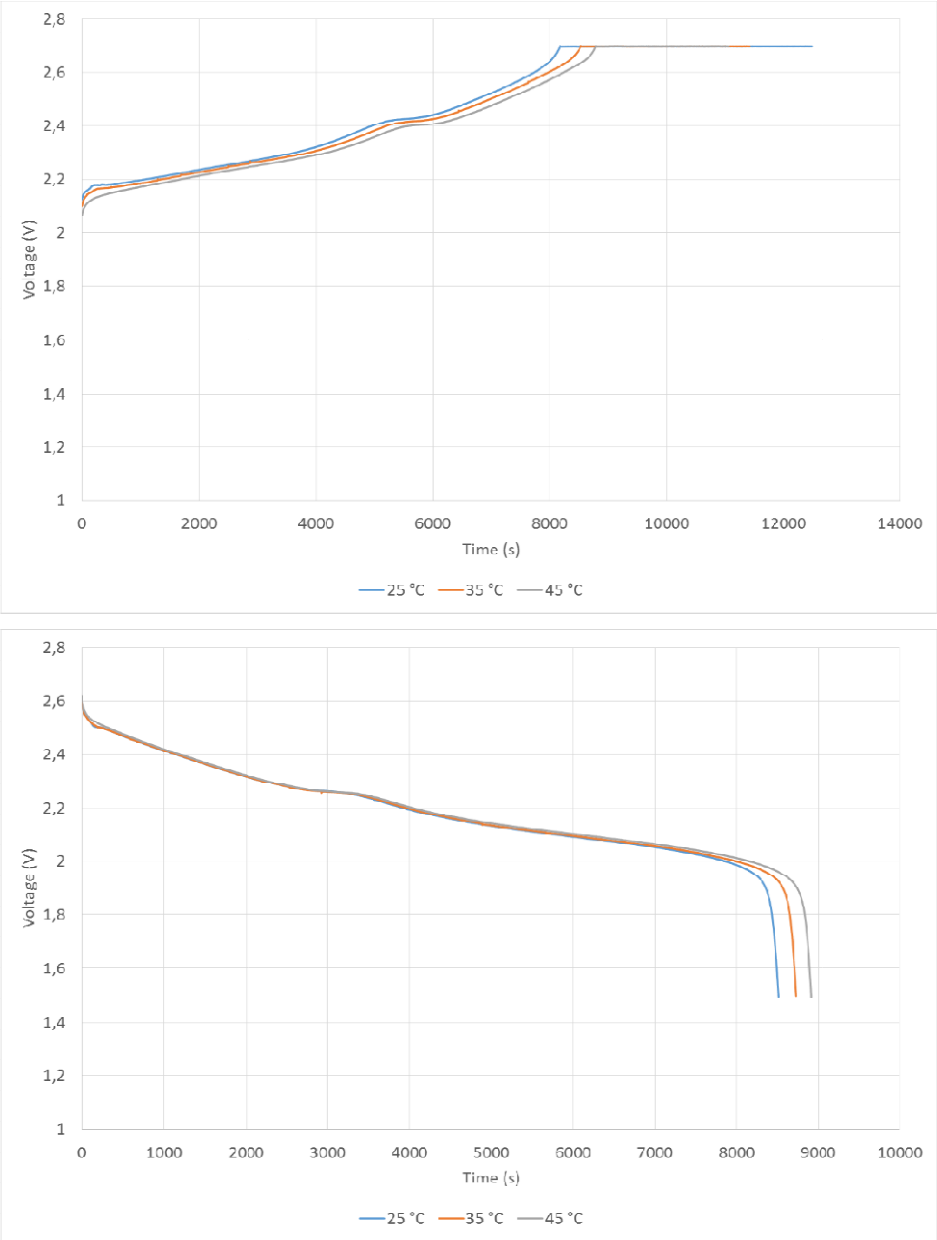

Figure 12 - Charge and discharge voltage profiles at different C-rate and 25 °C of the single cell

A slight variation of the voltage profile with the temperature was observed. This can be attributed to the modification of internal resistance of the cell and the different kinetic of redox reactions inside of that. As can be better observed from the discharge profile, although using the same c-rate, the time to reach the lower cut-off voltage increases as temperature increases. This suggests that the operating temperature can affect the discharge capacity of the cell.

Table 5 reports the measured discharge capacity as function of C-rate and different temperature. At 25 °C and 1 C, the measured capacity was 23.2 Ah, which matches with the nominal capacity declared by the manufacturer for this cell at the mentioned conditions. By decreasing the C-rate, the measured capacity showed a slight increase of its value as effect of an improved response of the cell to low discharge currents. Discharge capacity also showed a

slight increase of its value with increase of the temperature, which could be attributed to the favourable kinetic of redox reactions inside the cell.

Table 5 - Discharge capacity as function of temperature and C-rate

	1 C	0.75 C	0.5 C	0.25 C
25 °C	23.20 Ah	23.38 Ah	23.63 Ah	24.06 Ah
35 °C	23.83 Ah	24.00 Ah	24.23 Ah	24.61 Ah
45 °C	24.38 Ah	24.54 Ah	24.74 Ah	25.06 Ah

Further tests were then performed on the battery module. At first, it was conditioned by four charge-discharge cycles at 25 °C with the aim to stabilize the battery parameters. During this procedure the module was charged and discharged at constant current of 45 A (1 C) within the upper and lower cut-off voltages of 32.4 V and 18 V, respectively.

Voltage and current profiles recorded during this process are shown in Figure 13. The capacity of the module was evaluated as the maximum Ampere-hours discharged after this conditioning procedure. The measured value of 44.63 Ah is very close to the capacity declared by the manufacturer for this module.

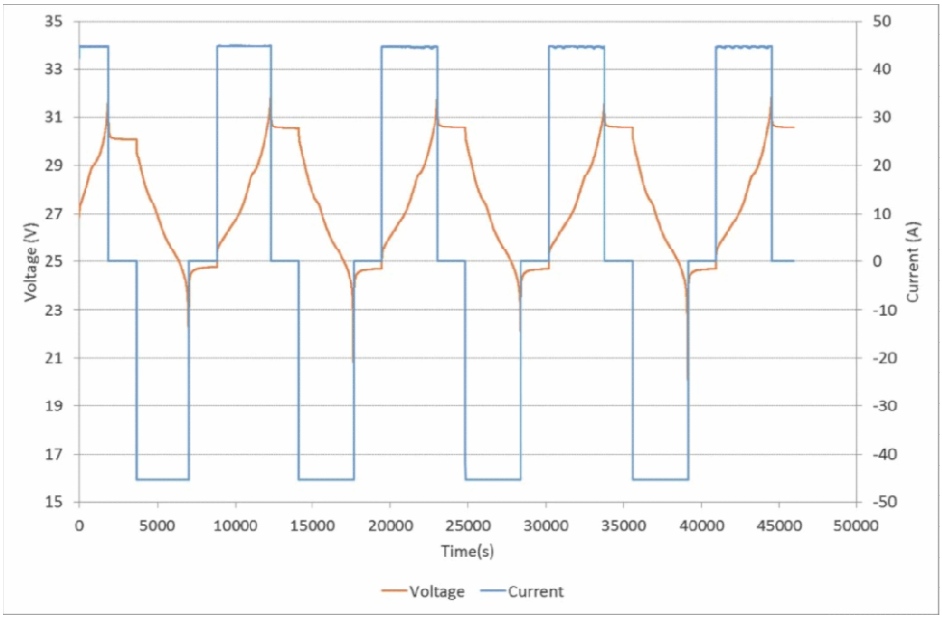

Figure 13 - Conditioning of the battery module

Figure 14 shows the voltage profiles of the battery module recorded during galvanostatic charges and discharges at different C-rates (1-0.5-0.25 C) and 25 °C. Charge and discharge tests were performed under CC mode until the upper and lower cut-off voltages (32.4 V and 18 V, respectively) were reached. As can be observed, the voltage profiles of the module at different C-rates, are very similar to those recorded for the single cell but scaled in magnitude due to the serial connection of multi-cells. Similarly to the single cell, slope variations of the voltage profiles, due to the phase transformation processes of anodic and cathodic materials as effect of lithium intercalation and de-intercalation from the electrodes, are also well visible for the battery module.

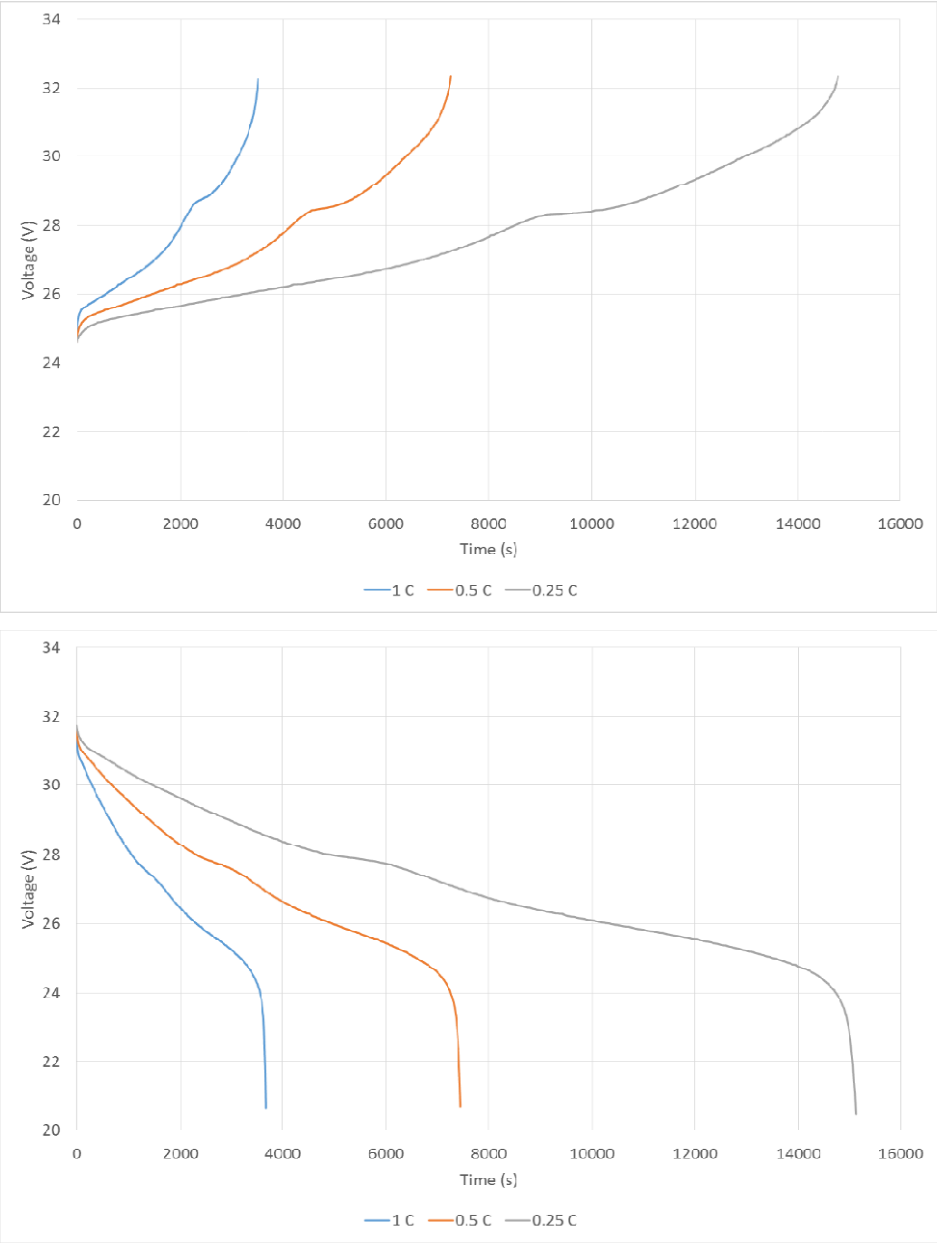

Figure 14 - Charge and discharge voltage profiles at different C-rate and 25 °C of the battery module

The performance of the battery module was also evaluated measuring and calculating the discharge energy and the energy efficiency at different C-rates, by a dedicated test. A charge protocol, consisting in multi-steps galvanostatic mode (1 C, 0.5 C, 0.2 C, 0.1 C and 0.05 C) each one of these up to the upper cut-off voltage and separated by 3 s rest phases, was used for this purpose. Galvanostatic discharge was carried out after 1 h rest from charge phases. The same protocol was then repeated for different discharge rates of 0.25 C, 0.5 C, 1 C and 2 C, respectively (Figure 15).

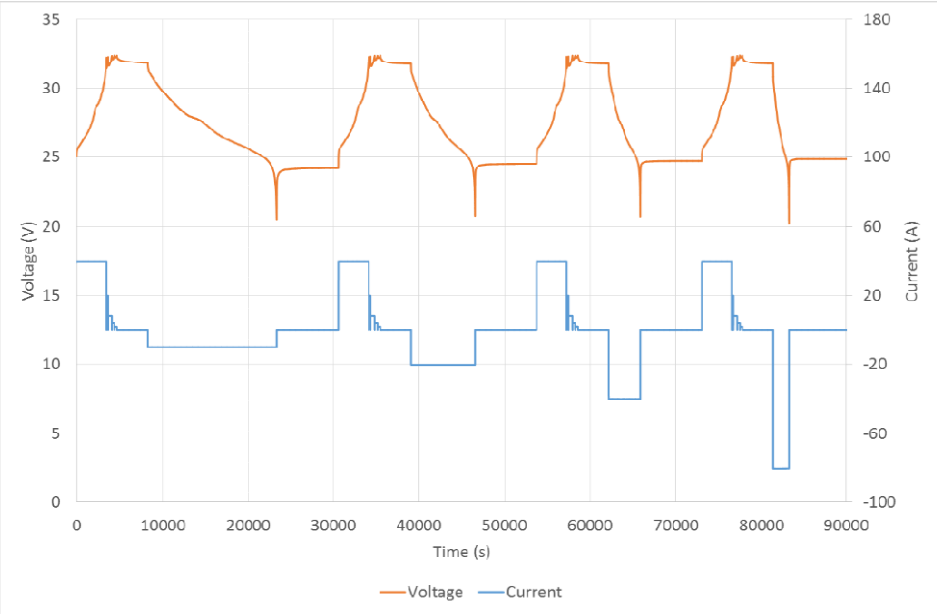

Figure 15 - Voltage and current profiles of the battery module at 1 C charge, different discharge C-rates and 25 °C

Discharge energy was calculated as the Watt-hours discharged from the upper voltage to the lower cut-off voltage of the module. Energy efficiency was defined as ratio between discharge energy (Wh) at different C-rates and cumulative charge energy (Wh) according to the above protocol. An excellent energy efficiency, ranging from 95 to 97 %, was obtained for the module at different C-rate from 2 C to 0.25 C (Table 6).

Table 6 - Discharge energy and energy efficiency as function of C-rate, of battery module

	Discharge Energy (Wh)	Energy efficiency (%)
0.25 C	1158	97,64
0.5 C	1133	97,42
1 C	1108	96,43
2 C	1083	95,08

For the life-time evaluation of the module an aging test at 25 °C was performed according to a defined current profile, which consisted of charge-discharge current steps at different C-rates.

The aging of the module was evaluated as loss of capacity during the days, as effect of the continuous operating of the battery under the defined current profile. Figure 16 shows the discharge capacity evaluated every ten days during the aging test. No loss of capacity has been observed over 210 days.

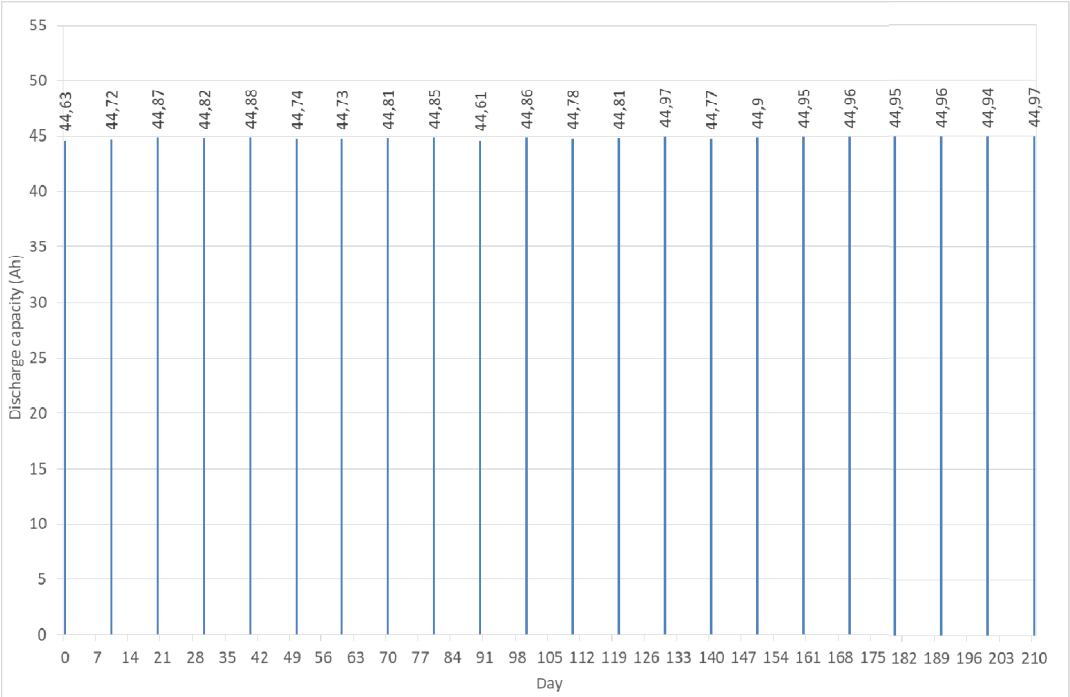

Figure 16 - Evolution of discharge capacity of the battery module during 210 days of ageing test

3.2 BMS adaptation

The BMS development involved both hardware and software implementation activities. Generally speaking, the main goal was the adaptation of the existing BMU (Battery Management Unit) / CMUs (Cell Management Units) signals exchange (process variables, alarm and failure states, hardware commands) and data structure to the PCS interface (to communicate with the new main controller). This goal implied to develop a system to bidirectionally convert data (i.e. implement the transcoding functions) among a CAN network (within the battery pack/unit) and the Modbus network mastered by the PCS.

3.2.1 Hardware development

In order to use commercially available hardware device, an Anybus converter by HMS (hereinafter referred as "gateway") was selected as the main device of the transcoding system. Beyond the CANbus and Modbus ports, this device has a USB programming interface to implement timing, control, and data management functions. In particular, the gateway internal memory management allows to temporarily store data coming from both data ports as well as write locations as bytes, words and double words to cope with different data length frames. What seems particularly important is the implementation of both periodic refresh/readouts beside the possibility of query (i.e. request / response) frames.

The overall control system and communication lines may be represented by the Figure 17.

Figure 17 - Schematic representation of the data exchange architecture from PCS (Modbus RTU) to BMU (proprietary CANbus) and viceversa, through a conversion gateway

The gateway exchanges CANbus frames with the BMU, and then it parses, splits, and re-arrange the process variables values into data structures compliant with the Modbus RTU. On the other hand, by acting as a Modbus slave, it receives data from the PCS Modbus line and assemble the data into the CANbus frames compliant with the BMU communication protocol by adding control / header information of the CANbus stream. The details of the operations are described in the software and firmware development paragraphs.

The communications protocol between the electric storage system and the controller is based on serial interface (HW/SW) consisting of a RS232 port and Modbus line.

Since the battery pack controller (Battery Management Unit, BMU) has a CANbus interface, a dedicated gateway "Anybus Communicator CAN Modbus RTU" by HMS (Figure 18) was necessary to:

- transcode data from CANbus frame to Modbus register (and vice versa),

- decouple the two networks (Modbus and CANbus) and, therefore, to allow asynchronous communications.

Figure 18 - Used gateway: Anybus Communicator CAN Modbus RTU

The (Modbus interface) serial communications settings are:

Communication line: 3-wire RS232 (it is possible to convert into 2-wire RS485 by physical switch), db9 female connector

Baud rate: 38400 bit/s (can be set differently, if necessary, by physical switches)

Parity: None (can be set differently, if necessary, by physical switches)

By physical switches, the Modbus slave interface of the gateway can be set on different ID to be inserted in complex systems/network (in our implementation the default ID = 5 was set)

3.2.2 Software development activity

The software development activity was addressed to implement the transcoding algorithm and the communication between the PCS (from CSEM) and the storage system (from CNR) by synthesize a common data structure description including the frame timing, signals priorities, system operation limitations to achieve a common FSM (Finite State Machine) implementation.

Given that the system controller operates Modbus (RTU) protocol, to describe the general data structure, the exchanged frames were divided according to the two transmission directions as readable data (BMS to PCS) and writable data (PCS to BMS) through the gateway.

Concerning with the former group, a list of 16 bit registers was implemented according to the following tables (i.e. the Modbus interface structure of the gateway) that explain the register content and the mapping of the data value (since each Modbus register is 16 bit long, divided into Most Significant Byte (MSB) and Least Significant Byte (LSB), addressed as follows):

Table 7 - Data content from battery pack/BMU to PCS

MB_reg# (DEC)	Data type	MSB	LSB
1	16 x 1 bit (coil)	Battery pack Status	Status additional information
2	16 x 1 bit (coil)	Charge/discharge complete	Operational limitations reached
3	UINT16	Battery pack State of Charge	
4	UINT16	Battery pack State of Health	
5	UINT16	Highest cell voltage in the battery pack	
6	UINT16	Lowest cell voltage in the battery pack	
7	INT8		Highest cell temperature
8	INT8		Lowest cell temperature
9	UINT16	Actual current (charge phase)	
10	UINT16	Actual current (discharge phase)	
11	UINT16	Battery pack voltage	
12	UINT8		SoC%
13	3 x 1 bit (coil)		Modules controllers failure

Table 8 - Mapping of the physical values in the registers (from battery pack to PCS)

System variables to Modbus registers mapping					
Register name	**Register#**	**type**	**unit**	**NOTES**	**equivalent coils**
Status	1	coils	MASK	see mask	16-23
Status_details	1	coils	MASK	see mask	24-31
EoC / EoD	2	coils	MASK	see mask	32-39
CellsAlarms	2	coils	MASK	see mask	40-47
absSoC	3	U16	mAh		
absSoH	4	U16	mAh		
maxCellV	5	U16	mV		
minCellV	6	U16	mV		
maxCellT	7	I8	°C	7bits and sign (msb)	
minCellT	8	I8	°C	7bits and sign (msb)	
cCurrent	9	U16	10 mA		
dCurrent	10	U16	10 mA		
unitVoltage	11	U16	0.1 V		
percentSoC	12	U8	%		
CMUsAlarms	13	coils	MASK	0 = no failure; see mask	208-210

In Table 7 and Table 8 both coils (i.e. digital/boolean signals) and holding registers are included to allow even a single reading operation and the consequent parsing process, or (with different modbus functions) the readout of a single bit or register.

However, to detect the single system status, cause of an alarm or failure, the tabled information must be completed with the following data map (Table 9):

Table 9 - Mapping of the Boolean content of status/alarm registers (from BMU to PCS)

	Coils map (first register + increment)				
increment	**Status (16)**	**Status details (24)**	**EoC / EoD (32)**	**CellsAlarms (40)**	**CMUAlarms (208)**
0	main contactor close	Low power	Close to EoC	Overcharge alert	Module01 fault
1	contactor close wait	Overcurrent	EoC reached	Overcharge fault	Module02 fault
2	leak detection ongoing	Shutdown permission	N/A	Overdischarge alert	Module03 fault
3	Unit ready	Pre-charge contactor (O/C)	N/A	Overdischarge fault	N/A
4	BMU failure	Leak detection	Close to EoD	OverT protection	N/A
5	Pre-charge abnormality	STOP detection	EoD reached	OverT alert	N/A
6	Leak detected	SDC state	N/A	N/A	N/A
7	Watchdog	Memory failure	N/A	N/A	N/A

To avoid the triggering of the alert/fault conditions, it was chosen to operate the battery system between 10%<SOC<90% only. When the limits are reached, the PCS should reduce the current accordingly to the actions foreseen in the table in the cases of EOC and EOD.

Similarly, the writable data frames to set variables such as the timestamp or to send commands (such as start/stop) and control signals (such as the watchdog to detect communications or PCS failure) were structured in 16 bit registers, as per required by the Modbus RTU standard.

Output variables are used to:

- send start/stop commands (as required at the start-up, in case of external alarms),
- battery pack voltage measurement (from PCS, to verify the measurement alignment and coherence),
- PCS presence signal (to bring the battery pack in “protection mode”, i.e. disconnection, in case of connection loss or PCS fault),
- A 64-bit timestamp to synchronize data for recording.

Table 10 and Table 11 report the output variables content and mapping, respectively.

Table 10 - Data content in writable registers from PCS to battery pack controller (Modbus interface)

MB_reg# (DEC)	**Data type**	**MSB**	**LSB**
1025	8 x 1bit (coil)	PCS signalling	
1026	UINT16	Battery pack voltage (external measurement)	
1028 - 1031	UINT16	timestamp	

Table 11 - Mapping of the physical values in the writable registers (from PCS to BMU)

System variables PCS to gateway / battery controller registers mapping					
Register name	**Register#**	**Type**	**unit**	**NOTES**	**equivalent coils**
timeWord#1	1031	U16		64 bit timestamp (system initialization)	
timeWord#2	1030	U16			
timeWord#3	1029	U16			
timeWord#4	1028	U16			
writeStatus	1025	U8 in U16		See Table 12	16400 - 16407
systemVoltage	1026	U16	0.1 V	system initialization	

Even in this case, the writeStatus byte require a mapping mask to specify the meaning of each single bit:

Table 12- Mapping of the Boolean content of the control register (from PCS to BMU)

increment	**writeStatus (coils offset = 16400)**
0	STOP=0 / START=1
1	Power failure
2	Not used
3	Not used
4	N/A
5	N/A
6	N/A
7	Watchdog

To develop the FSM, a description of the procedures triggered by the single status/error/alert/fault coil commutations was approached. At the beginning, the meaning of each coil was considered and summarized by a table of possible cases and distinguishing the irreversible faults from alert states, system limitation states, and normal operation.

In Table 13, the correspondence between each bit of each byte in the first two Modbus registers (#01 and #02, 16 bit) with:

- Red: warning/fault and suggested action;
- Purple: small margin / alert conditions and suggested action;
- Green: Initialization and shutdown states/permission/indications;
- Blue: periodic checks;
- Black: other information.

Table 13 - Mapping of the Boolean content of the status/alarm registers (from BMU to PCS) with required reacting actions / warning countermeasures / system status representation

A	B	C	D
01_MSB	01_LSB	02_MSB	02_
STATUS	STATUS DETAILS	EOC EOD	OVER_
in contactor state	**Low power mode**	**Close to End of Charge**	**Overcha**
0: open	*0: CMU power on*	*0: normal*	*0: nc*
1: closed	*1: CMU power off*	*1: reduce charging current (<45A if room temperature < 15°C)*	*1: wait 30 minu try to disch * contact*
ntactor waiting status	**Overcurrent**	**End of Charge**	**Overcha**
0: no wait	*0: normal*	*0: normal*	*0: nc*
1: wait for close	*1: reduce battery current * contactor is open*	*1: STOP charge: only discharge permitted*	*1: stop syst*
N/A	**BMU shutdown permission**	N/A	**Overdisch**
	0: not permitted		*0: nc*
	1: waiting for shutdown		*1: wait 30 minu try to recha * contact*
Init preparation	N/A	N/A	**Overdisch**
0: not prepared			*0: nc*
1: prepared			*1: stop syst*
MU abnormality	N/A	**End of Discharge**	**High temperat**
0: OK		*0: normal*	*0: nc*
1: call ITAE		*1: STOP discharge: only charge permitted*	*1: suspend battery*
N/A	N/A	**Overdischarge warning**	**Overtempe**
		0: normal	*0: nc*
		1: try charge battery (within 1h): if impossible turn off BMU. Re-charge battery within a week	*1: suspend battery u reset s * contact*
N/A	N/A	**Close to End of Discharge**	N
		0: normal	
		1: reduce discharge current (<45A if room temperature < 15°C)	
Watchdog	**Memory failure**	N/A	N
riodic commutation (960ms)	*0: normal*		
t 3 seconds: restart system			
imes: stop system, call ITAE	*1: STOP, call ITAE*		

Once completed this description of the possible state transitions conditions, the procedures to cope with each case were defined.

In details, this was done by assigning and identified to each case through the following procedure:

In the table, the columns (each one associated to a letter A, B, C, and D) represent the single byte within the holding /reading) registers #01 and #02 and the rows represent the bit position in the single byte (0 to 7, from LSB to MSB).

In particular, the columns can be described by:

A: register 01, most significant byte (STATUS);

B: register 01, least significant byte (STATUS DETAILS);

C: register 02, most significant byte (EOC EOD);

D: register 02, least significant byte (OVER_LIMITS);

0-7 is the bit in a single “lettered” byte.

Provided this convention, each status bit can be referred by a letter+number combination (e.g.: A3 = unit preparation; C6 = close to End of Discharge) and indicates (except for the “N/A” cells) a system status condition (normal operation, alert, failure, power limitation, and so on) and (if required) the procedure to start.

In details, the 32 cells of the table can be divided in:

12 cells (**A2, A5, A6, B3, B4, B5, B6, C2, C3, C7, D6, and D7**) unused.

B0: only to know if the CMUs are idle (minimum power consumption).

A7: is the heartbeat / life signal / watchdog bit (that must be cyclically commutated 0->1->0).

In the following procedures, a graphic convention to distinguish (for instance) assignment from comparison instructions, so that:

“==”, “>=” are comparison operators;

“:=” is assignment (value to variable or name to system state);

“||” is Boolean OR;

“&&” is Boolean AND;

“=” is initial state of the described transition.

Moreover, since a single cell could trigger different actions, the sequence

xxxxxxxxxxxxxxxxxxxxxxxxxxxxxxxxxxxxxxxxxx

is the separation of different initial states / transitions for a single bit/cell of the table (i.e. different cases for the same bit).

Furthermore, to distinguish automatic procedure from manually managed conditions, the following convention was adopted:

Green font for automatic actions;

Red font for manual actions;

Blue font for actions that can be implemented in automatic mode, but human supervision could be useful at least in the initial tests and trials.

Provided the conventions/glossary above, five cells indicate (irreversible) fault conditions, so that it was chosen to operate manually with deep diagnostic (this is indicated as “Call ITAE”)

A4 (BMU abnormality), B7 (memory failure), D1 (overcharge fault), D3 (overdischarge fault), C5 (overdischarge warning):

STATE = NORMAL OPERATION

If (bit=TRUE) then {

Send STOP;

Call ITAE

}

STATE := FAULT

A1 (main contactor waiting status), A3 (unit preparation):

STATE = IDLE

If (A3=TRUE) && (A1=TRUE) && (you want to start the system = TRUE) then

Send START;

STATE := Normal operation

xxxxxxxxxxxxxxxxxxxxxxxxxxxxxxxxxxxxxxxxxxx

STATE = IDLE

If ((A3=FALSE) || (A1=FALSE)) && ((any fault = TRUE) || (any warning = TRUE) && (A0 = FALSE) then Call ITAE;

STATE := FAULT

xxxxxxxxxxxxxxxxxxxxxxxxxxxxxxxxxxxxxxxxxxx

NOTE: The remaining condition, i.e. (A1 or A3 false) AND “no warnings” is a temporary state that should last about 5.5s

---

B2 (BMU shutdown permission):

STATE = NORMAL OPERATION

If (B2=TRUE) && (you want to shutdown the system) then Send STOP;

STATE := STOP

xxxxxxxxxxxxxxxxxxxxxxxxxxxxxxxxxxxxxxxxxxx

STATE = NORMAL OPERATION

If (B2=FALSE) then “do not switch off the BMU”

D5 (overtemperature alert):

STATE = NORMAL OPERATION

If (D5 = TRUE) then Send STOP; → STATE := OVERTEMPERATUREALERT

Wait until < 40°C, then "Reset the system" → *STATE := IDLE*;

B1 (overcurrent) - indeed this bit will always be FALSE, since the overcurrent threshold (220A) is higher than the DC/DC maximum value (80A):

STATE = NORMAL OPERATION

If ((B1=TRUE) && (A0=1)) then *"reduce current"*;

xxxxxxxxxxxxxxxxxxxxxxxxxxxxxxxxxxxxxxxxxxxx

STATE = NORMAL OPERATION

If ((B1==TRUE) && (A0=0)) then "reset the system";

STATE := IDLE

C0 (close to end of charge):

STATE = NORMAL OPERATION

If (C0==TRUE) then {

If (room temperature >= 15°C) then *"reduce charging current set-point"* else *"reduce charging current set-point below 45A"*;}

C6 (close to end of discharge):

STATE = NORMAL OPERATION

If (C6==TRUE) then {

If (room temperature >= 15°Cwa) then *"reduce discharging current set-point"* else *"reduce discharging current set-point below 45A";*}

C1 (end of charge):

STATE = NORMAL OPERATION

If (C1==TRUE) then "current set-point only discharge allowed";

STATE := CHARGELIMITED

xxxxxxxxxxxxxxxxxxxxxxxxxxxxxxxxxxxxxxxxxxxx

STATE = CHARGELIMITED

If (C1==FALSE) then "current set-point within normal span";

STATE := NORMAL OPERATION

C4 (end of discharge):

STATE = NORMAL OPERATION

If (C4==TRUE) then "current set-point only charge allowed";

STATE := DICHARGELIMITED

xxxxxxxxxxxxxxxxxxxxxxxxxxxxxxxxxxxxxxxxxxxx

STATE = DICHARGELIMITED

If (C4==FALSE) then "current set-point within normal span";

STATE := NORMAL OPERATION

D4 (overtemperature protection):

STATE = NORMAL OPERATION

If (D4==TRUE) then "current set-point = 0A";

STATE := OVERTEMPERATUREPROTECTION

xxxxxxxxxxxxxxxxxxxxxxxxxxxxxxxxxxxxxxxxxxxx

STATE = OVERTEMPERATUREPROTECTION

While (Register_07.MSB >= 40°C) do {wait 1 second}

STATE := NORMAL OPERATION (➔current set-point recovers normal span)

D0 (overcharge alert):

STATE = NORMAL OPERATION

IF (D0==TRUE) then Send STOP;

STATE := OVERCHARGEALERT

xxxxxxxxxxxxxxxxxxxxxxxxxxxxxxxxxxxxxxxxxxxx

STATE = OVERCHARGEALERT

"Wait for 30 minutes";

"reset the system";

If ("any_fault" == TRUE) || ("any_alert" == TRUE) then {

STATE := OCFAULT;

call ITAE;

}

else {

"discharge the battery";

STATE := NORMAL OPERATION;

}

D2 (overdischarge alert):

STATE = NORMAL OPERATION

IF (D2==TRUE) then Send STOP;

STATE := OVERDISCHARGEALERT

xxxxxxxxxxxxxxxxxxxxxxxxxxxxxxxxxxxxxxxxxxx

STATE = OVERDISCHARGEALERT

"Wait for 30 minutes";

"reset the system";

If ("any_fault" == TRUE) || ("any_alert" == TRUE) then {

STATE := ODFAULT;

call ITAE;

}

else {

"charge the battery";

STATE := NORMAL OPERATION;

}

A0 (main contactor status): it is used in combination with other status/control bits above described. However, it is used to verify:

- the START/STOP command sent by your PCS was received by the BMU;
- the intervention of the BMU in case of alert (as above indicated)

From this list of procedures, a first tentative FSM was obtained.

The FSM implements 6 system states (among them, one is dedicated to defining all the fault conditions regardless the triggering cause), as in the following list:

IDLE: system powered on with BMU powered off;

INIT: transient after BMU power on (internal procedure/checks);

READY: BMU waits for start signal;

NORMAL OPERATION: system is working;

STOP: stop signal was sent, waiting for BMU power off;

FAULT: BMU detected malfunctioning (external actions to remove fault are required)

The graphic representation of the states-and-transitions scheme is represented by the Figure 19 (the entry action of each state is reported within the related circle):

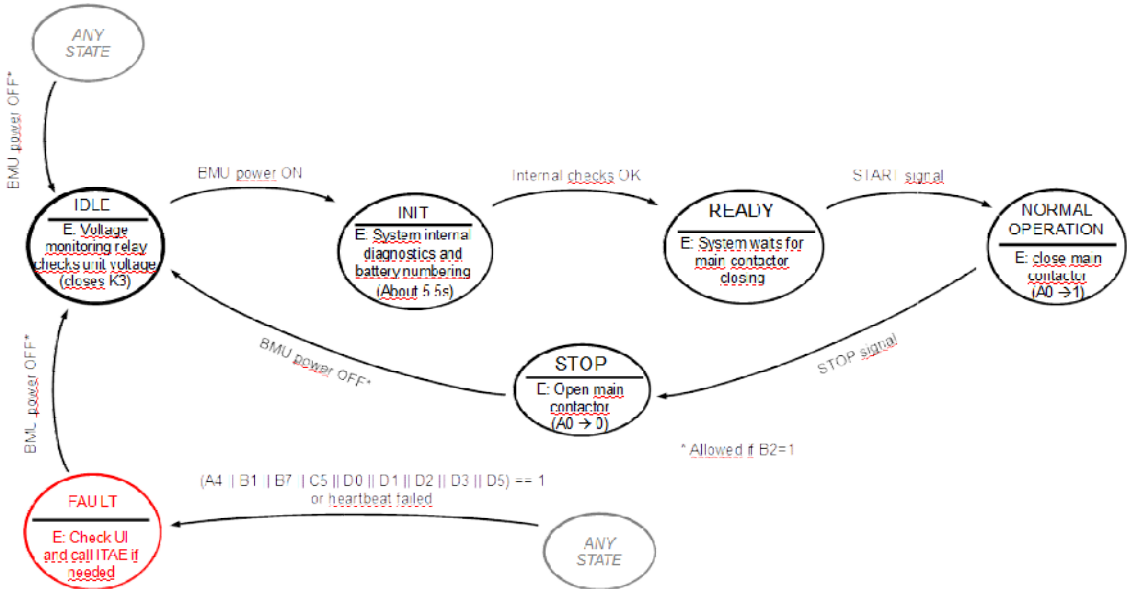

Figure 19 - Representation of the developed FSM: it includes system states, triggering transition conditions, and entry actions.

3.2.3 Firmware development

For the firmware development, the gateway memory is split into three addressable areas dealing with the Modbus network, the CANbus network (subnetwork according to the manufacturer naming), and a general purpose area for internal manipulation procedure (not used in this application).

In this implementation, to optimize the memory arrangement (despite by far larger than the requested data amount), the areas were segmented into contiguous blocks depending on the data size (coils, bytes, words) and a simplified fetching from the PCS was assured.

For example, the 4 timestamp words (i.e. 64bit) were positioned (in blue in Figure 20) in a single row (0x208 to 0x20F). Incidentally, in the same figure, two 8-bit counters were added (to avoid the waste of CANbus frame, for diagnostic/debug purpose only) as well as the two bytes highlighted in green available for the gateway diagnostic.

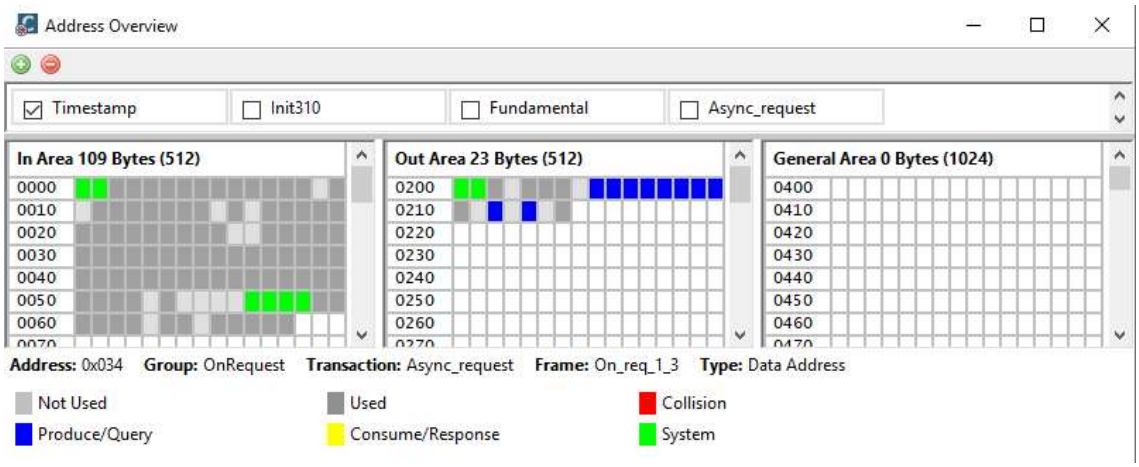

Figure 20 - 64 bit Timestamp memory allocation in the modbus frame (0x208 ts_lo_dword to 0x20F ts_hi_dword)

Similarly, the cyclic reading Modbus register (from gateway to the PCS) were adapted to be reached even in a single reading instruction (from location 0x02 to 0x031, in yellow). As per above explained for the timestamp counters, the extra yellow locations were used to temporarily store the cyclic frame counters of the CANbus frame (Figure 21).

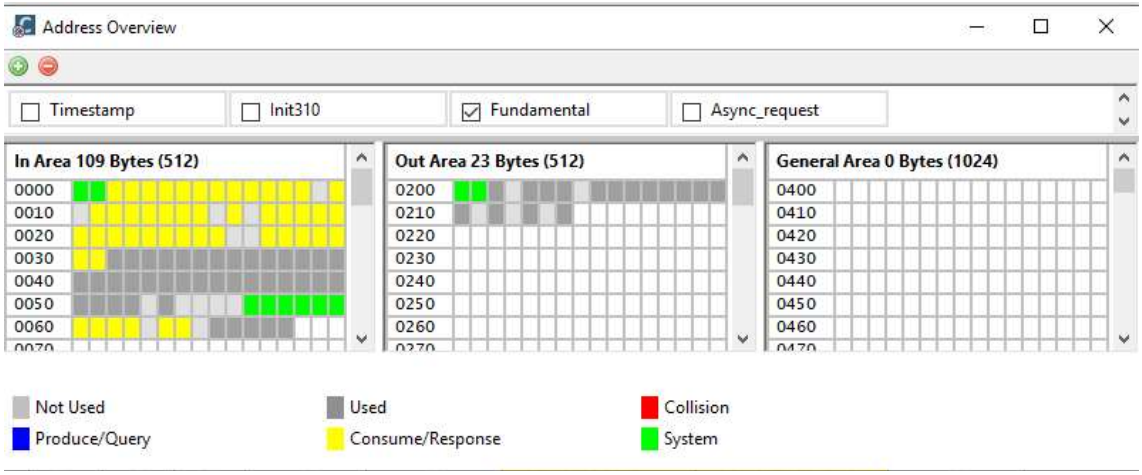

Figure 21 - System data values memory allocation in the modbus frame (0x0002 to 0x0032)

3.3 Battery system development and test in the lab

The whole storage system was wired to realize the prototype for testing and debugging of the control software (Figure 22). A 12V power supply was used for the BMU electronics and the equipment selected for CAN to MODBUS RTU conversion. The BMU system also required a current sensor (hall-effect type) mounted on the storage system power line and an external contactor directly managed by itself in case of fault conditions. The current sensor communicates with the BMU with an own internal CAN line. BMU also needed an external switch for reset, able to restart the same when fault conditions are reached. This external switch has to be controlled by the overall system supervisor: hence, CNR and CSEM have agreed to give the control of this switch to the external supervisor so obtaining a total control of the storage system in any operating case.

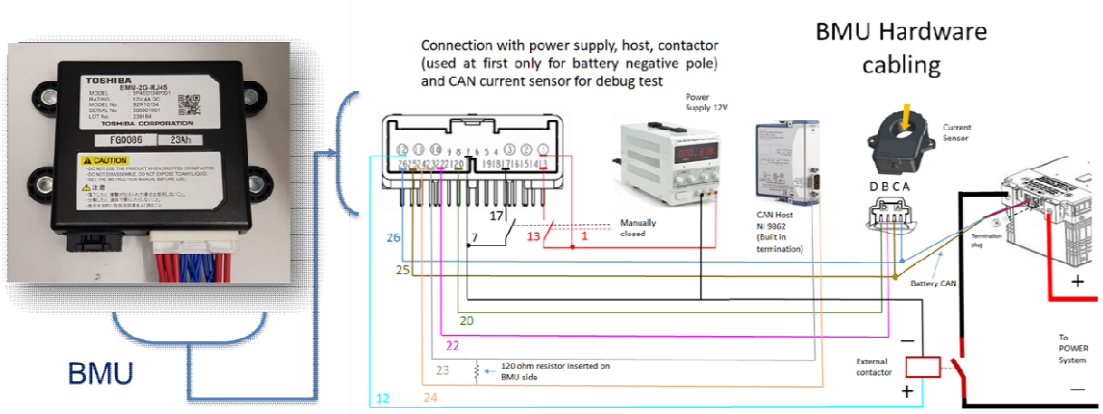

Figure 22 – BMU cabling

The storage system is composed by three modules mounted in series, as visible in Figure 23

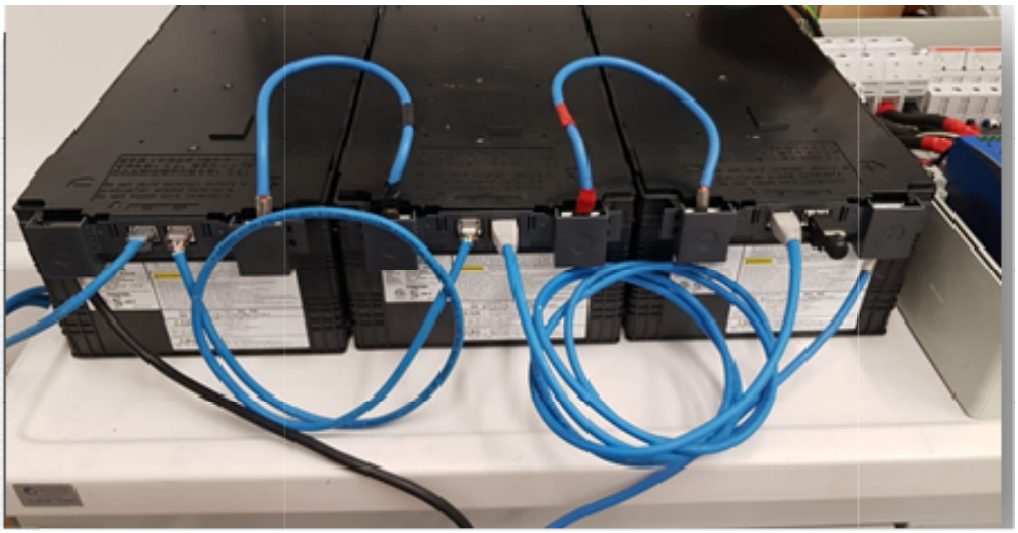

Figure 23 – Three LTO modules power and communication connections

In the final system, they will be connected to a DC link in which a dedicated DC/DC converter will impose the current set point (for charge and discharge) following selected algorithm decisions.

The electrical layout, including BMS interfaces, power suppliers, wiring, switches and connections was developed in order to achieve a final picture for the installation into a cabinet.

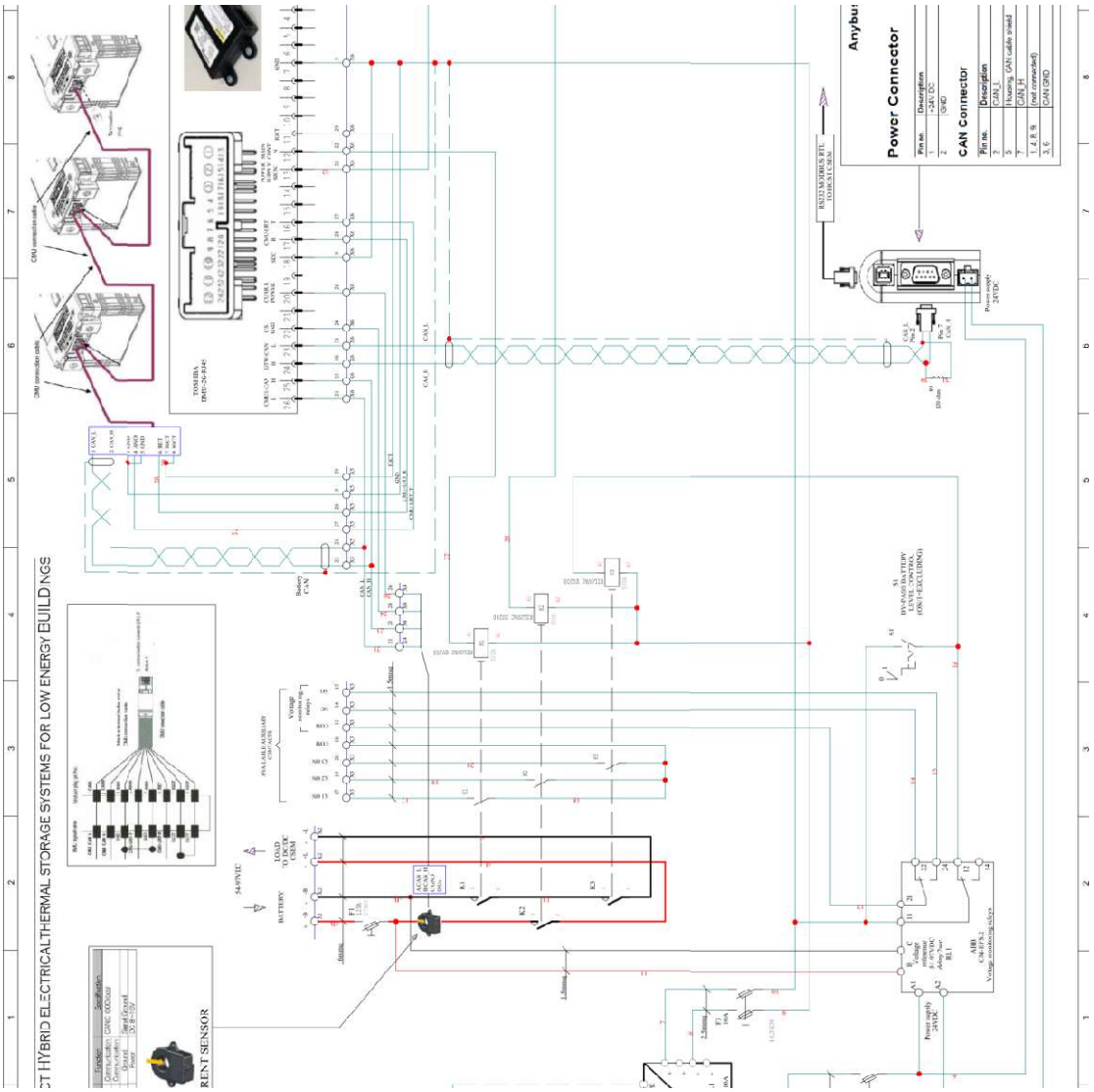

Figure 24 - Electrical layout of the battery system developed at CNR-ITAE

The first test on the whole pack was performed considering the worst scenario in the Mediterranean location selected, Cyprus, corresponding to a summer day (July) with very high demand coming from the cooling system and also a high PV production during the day. The test starts at 4:00 PM, when the battery is considered totally charged (90% SoC, since battery works between 90 and 10% SoC). This situation showed that PV production is able to charge the battery system very quickly, thus serving other loads or feeding the grid for long periods in the 24 hours observation window. During low production periods and night, the storage system discharges (about 8 hours after 4:00 PM) the energy stored during the relevant production period until fully discharging. It can be noted that, as expected in the worst operating conditions, there is no great coupling between PV production and storage because the former exceeds the capacity of the latter. The total PV excess (net of load request) is about 16kWh for the whole day, while the load not covered directly by the PV sums up to 6 kWh. In the whole day, the energy flowing through the batteries is about 3.5 kWh, i.e. about 56% of the net load request by time-shifting the PV excess.

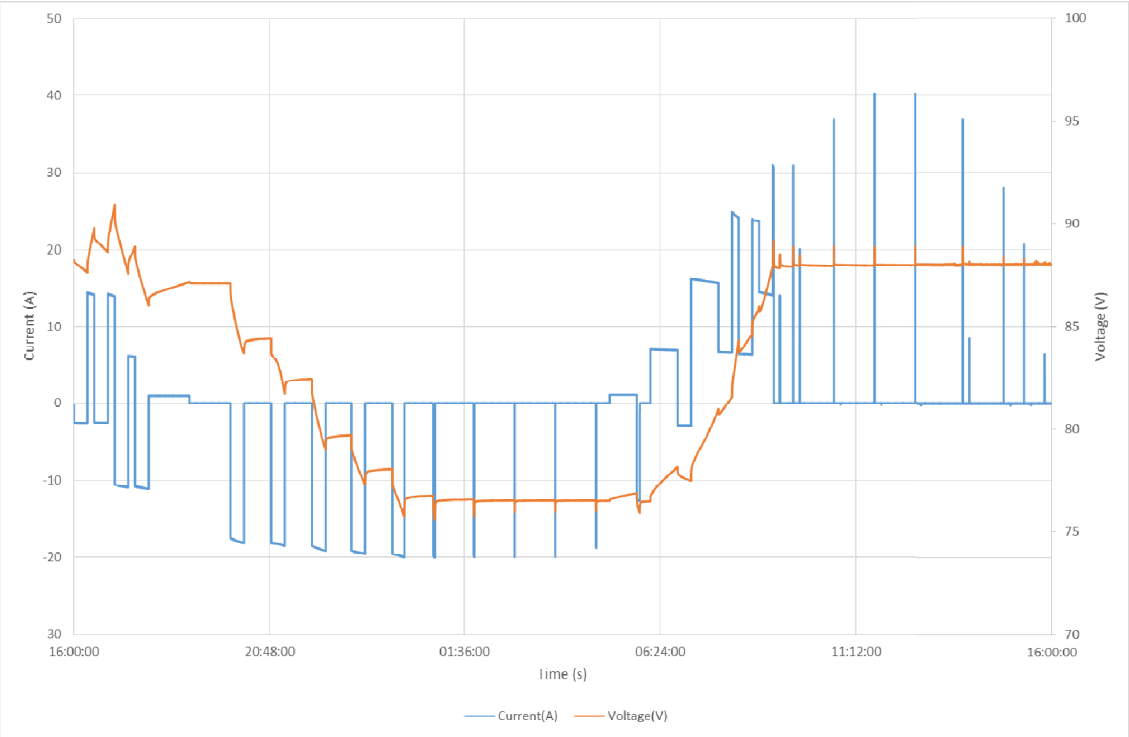

Figure 25 – Voltage and Current behaviour during the day (Cyprus, July)

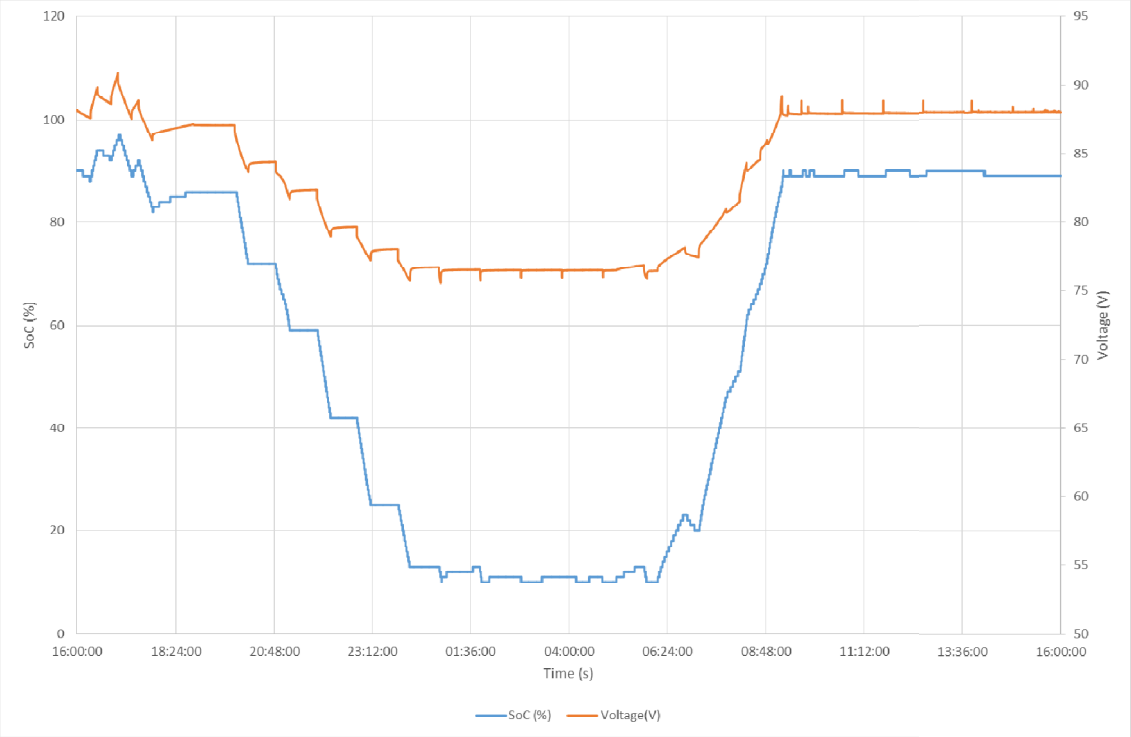

Figure 26 - Soc and Voltage variations during Mediterranean cycle (SoC is recorded by the BMU)

The second scenario describes a winter day in Bordeaux (the location chosen for the Continental case), where low irradiation (and therefore lower production from the PV field) and higher user demand were measured. Figure 27 shows that almost all the PV production excess is stored in the batteries but the daily power request consumes it in about 7 hours after reaching the fully charging condition. In this case, the test starts at 1:40 PM, corresponding to the first discharging request, after fully charging condition reaching. With the selected PV size,

the coupling with storage system is quite good: the net PV production (net after deducting the load request) is about 5.8 kWh, whereas the energy not directly supplied to the load by the PV is about 9.9 kWh (within the whole day). The net energy flow sums up to 3.7 kWh, i.e. 62% of the excess energy is used for time-shifting. However, due to the high load demand, the storage accounts only for 40% of the load request. This is related to PV size and only as a consequence to the storage. By increasing PV and battery size load supply can be improved.

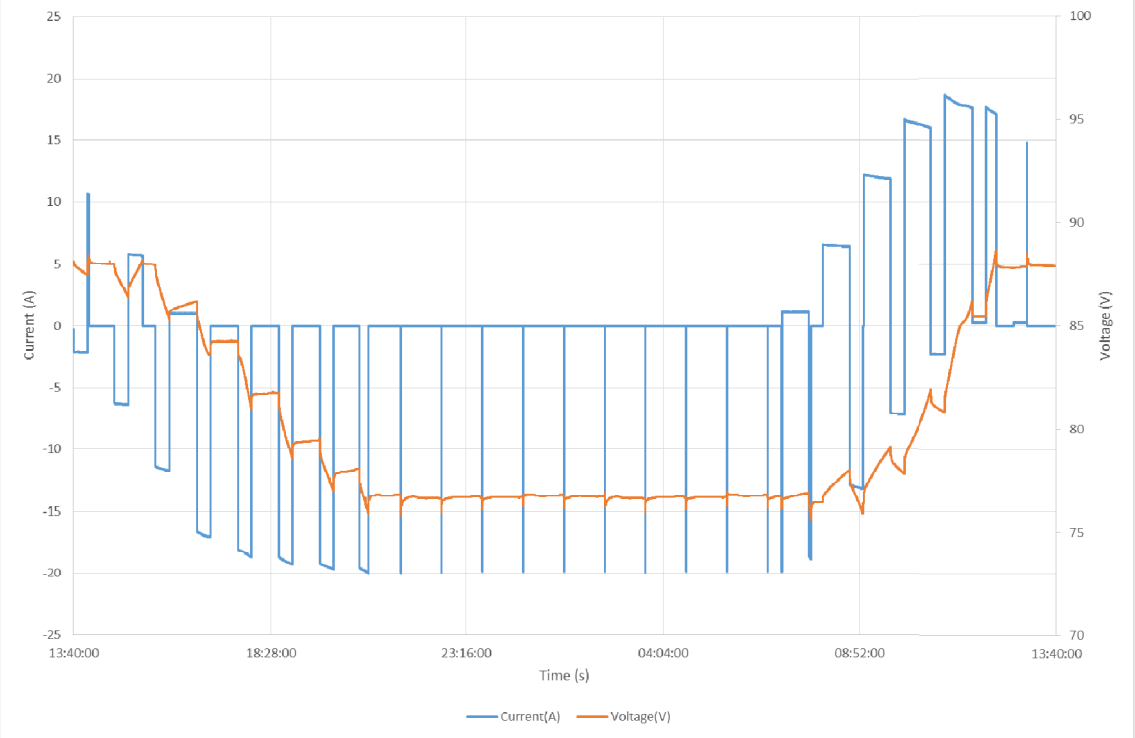

Figure 27 - Voltage and Current behaviour during the day (Bordeaux, January)

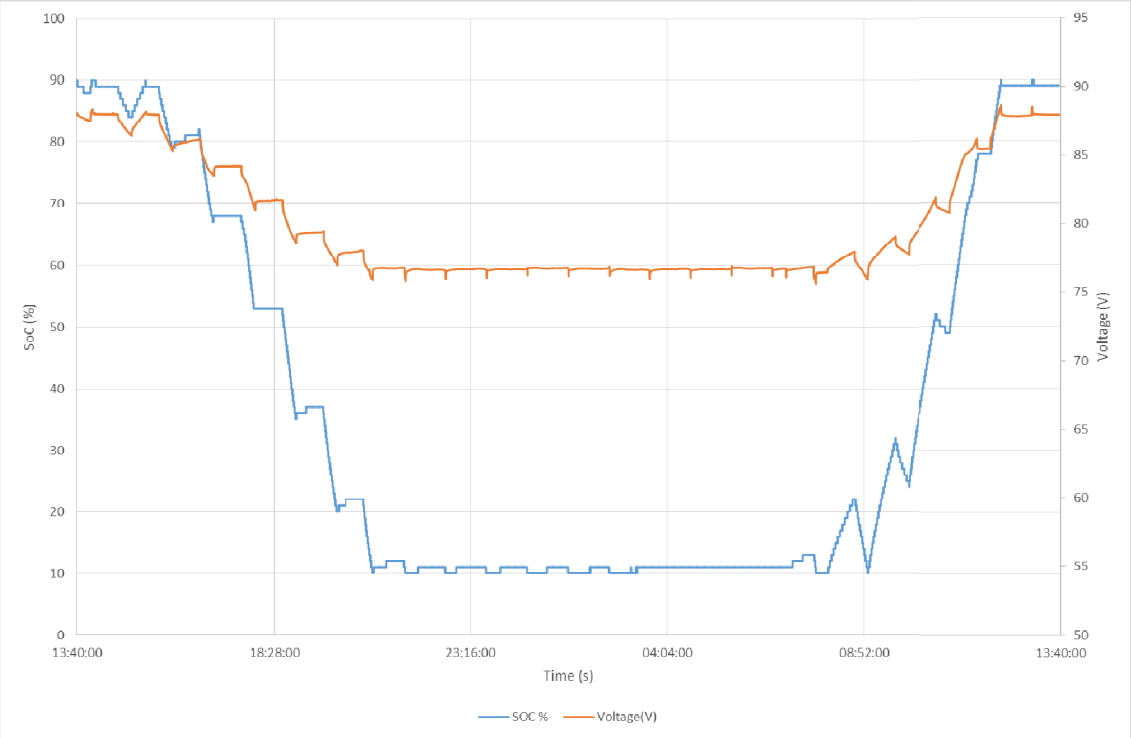

Figure 28 - Soc and Voltage variations during Continental cycle (SoC is recorded by the BMU)

The average temperature recorded during the cycles is 27 °C, as showed in Figure 29.

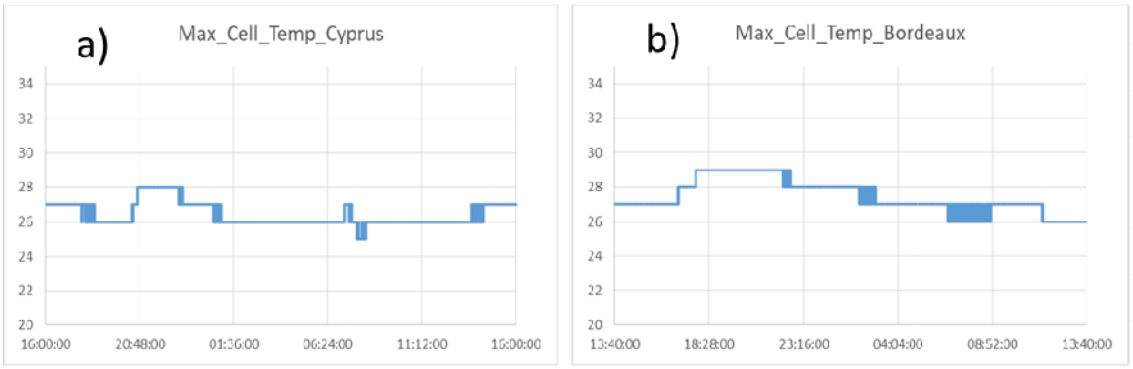

Figure 29 Temperature recorded during the simulated cycle, Figure a) Cyprus, Figure b) Bordeaux

A small electrical cabinet was chosen together with CSEM to ensure right protections (fuses, contactors) to the storage system for testing the DC-Link with CSEM and for achieving a final device to install into the demos, as reported in D2.3.

In particular, a further external protection system, which bypasses the BMU, was integrated to hold the operation voltage inside the rated maximum and minimum thresholds. This was done by using a voltage-controlled coil, which operates a dedicated contactor in case of exceeding the above-mentioned thresholds. The intervention of this protection system does not depend on the BMU control, ensuring safe operation even in case of BMU or communication failures.

The input of the designed electric cabinet can be directly connected with CSEM electric architecture, which provides also a necessary pre-charge device to avoid dangerous voltage discrepancy between the converter and the storage system.

4 Conclusions

This report summarizes the activities performed to develop and test the electric storage for the HYBUILD system. Among the lithium batteries technologies available on the market, Lithium Titanate Oxide chemistry was chosen. This choice is due to lifetime comparable with the typical working life of PV systems, very high safety, required for installation in building applications and high charge and discharge C-rates, thus enabling the system for different types of services (energy and power), also for on/off heat pumps. The design, realization and, test of the storage system were performed, from both electrical, mechanical, and control points of view. BMS adaptation and communication interfaces were debugged to obtain the full control of the storage system from the supervisor. Test campaigns conducted at cell, module, and pack level showed good agreement with the desired features. In particular, test conducted in climatic chamber at high temperatures showed a very good safety and performance recorded, also up to 45°C. The complete battery pack was tested also under real conditions, simulating both production from PV (in Cyprus and Bordeaux) and load profiles from the heat pump. The results showed a good rate of self-consumption due to the battery storage (56%-62%) and a very low average temperature of operation (27 °C), resulting in very safe conditions of operation.

5 References

[1] https://setis.ec.europa.eu/system/files/Technology_Information_Sheet _Electricity _Storage_in_the_Power_Sector.pdf

[2] N. Nitta, F. Wu, J. T. Lee, and G. Yushin, "Li-ion battery materials: present and future," Materials Today, vol. 18, pp. 252-264, 2015.

[3] J. Lu, Z. Chen, F. Pan, Y. Cui, and K. Amine, "High-Performance Anode Materials for Rechargeable Lithium-Ion Batteries," Electrochemical Energy Reviews, vol. 1, pp. 35-53, 2018.

[4] American Bureau of Shipping, Advisory On Hybrid Electric Power Systems, 2017. www.eagle.org.

[5] S. Lemon and A. Miller, Electric Vehicles in New Zealand: Technologically Challenged?, 2013.

[6] Qnovo, The cost components of a lithium ion battery, https://qnovo.com/82-the-cost-components-of-a-battery/." 2016.

[7] Recharge, Safety of lithium-ion battery, The European Association for Advanced Rechargeable Batteries, https://www.rechargebatteries.org/wp-content/uploads/2013/07/Li-ion-safety-July-9-2013-Recharge-.pdf. 2013.

[8] P. Röder, N. Baba, and H. D. Wiemhöfer, "A detailed thermal study of a $Li[Ni_{0.33}Co_{0.33}Mn_{0.33}]O_2/LiMn_2O_4$-based lithium ion cell by accelerating rate and differential scanning calorimetry," Journal of Power Sources, vol. 248, pp. 978-987, 2014.

[9] A. W. Golubkov, D. Fuchs, J. Wagner, H. Wiltsche, C. Stangl, G. Fauler, G. Voitic, A. Thaler, and V. Hacker, "Thermal-runaway experiments on consumer Li-ion batteries with metal-oxide and olivin-type cathodes," RSC Advances, vol. 4, pp. 3633-3642, 2014.

[10] J.-S. Park, S.-M. Oh, Y.-K. Sun, and S.-T. Myung, "Thermal properties of fully delithiated olivines," Journal of Power Sources, vol. 256, pp. 479-484, 2014.

[11] S. Lemon and A. Miller, Electric Vehicles in New Zealand: Technologically Challenged?, 2013.

[12] "https://batteryuniversity.com/learn/article/types_of_lithium_ion," 2019.

[13] F. Sergi, A. Arista, G. Agnello, M. Ferraro, L. Andaloro, and V. Antonucci, "Characterization and comparison between lithium iron p hosphate and lithium-polymers batteries," Journal of Energy Storage, vol. 8, pp. 235-243, 2016.